



Water Security
Agency 

Estevan Valley Aquifer
Development of a Regional Numerical Model

By
Anatoly Melnik, Hydrogeologist
Kei Lo, Manager, Groundwater Services

May 2018

© 2018, Water Security Agency.

The information contained in this report is provided as a public service by Water Security Agency,
101-111 Fairford Street East, Moose Jaw, Saskatchewan, Canada S6H 7X9.

Water Security Agency is not responsible for any errors or omissions, or for the results obtained from the use of the information contained in this report. The information contained in this report is provided “as is”, with no guarantee of completeness, accuracy, timeliness or of the results obtained from the use of this information, and without warranty of any kind, express or implied, including, but not limited to warranties of performance, merchantability and fitness for a particular purpose. Nothing herein shall to any extent substitute for the independent investigations and the sound technical and business judgment of the reader. In no event will Water Security Agency, its employees or agents, or the Government of Saskatchewan, be liable for any decision made or action taken in reliance on the information in this report or for any consequential, special or similar damages, even if advised of the possibility of such damages.

Executive Summary

The Estevan Valley Aquifer (EVA) is located north-west of the City of Estevan. It is a relatively narrow, and long (> 100 kilometres) paleo-valley consisting of interbedded sand, gravel, silt, and clay at depths of 50 to 150 m below ground surface. Although it has been mapped and explored since the late 1950s, its long-term yield remains unclear. SaskPower pumped this aquifer between 1988 – 1994 at average rate of 4,143 dam³/year and produced extensive drawdowns throughout the entire aquifer and across the international border. Aquifer behaviour showed that previous investigations have over-estimated the long-term sustainable yield.

A numerical groundwater model was developed herein to assist WSA staff in assessing the availability of groundwater resources in the EVA and predicting groundwater response from various pumping scenarios. The numerical model was developed using updated geological and hydrogeological information including testholes, piezometers, production wells, withdrawal data, and water level measurements incorporating an updated geologic framework.

Model development redefined our understanding of the EVA hydraulics. Specifically, the model suggests that the bulk vertical hydraulic conductivity (K'_v) of the overlying till likely ranges between 10^{-11} – 10^{-12} m/s, which is at least two orders of magnitude lower than previously considered for this area. The low K'_v implies that minimal vertical recharge is originating from the overlying till to the EVA. It further suggests that the major contribution of recharge is occurring laterally from the Eastend-Ravenscrag Aquifer. The Eastend-Ravenscrag Aquifer is likely recharged by vertical flow through the overlying thinner tills and from upland areas or along limited outcrops in the southern parts of the study area. The discharge area of the EVA remains unknown.

The model was calibrated and tested using various pumping scenarios. Transient calibration has shown that model is capable of adequately simulating stresses through most of the EVA, except in the Yellowstone Channel at the international border where errors were greater than in other parts of the aquifer. The calibration result at the international border is likely due to uncertainties in geology and the associated boundary conditions. The long-term sustainable yield was estimated to be between 1,200 – 2,100 dam³/year. However, the transient simulations showed that the aquifer could be pumped at greater rates for shorter periods. The transient model can provide an initial estimate of the expected drawdowns for any requested allocation assuming that the duration of withdrawal is known.

Table of Contents

Executive Summary

1.0	Introduction	1
1.1	Historical Investigations	2
2.0	Data and Methods	6
2.1	Study Area	6
2.2	Geological and Hydrogeological Information	6
2.3	Data Processing	7
2.3.1	Data Preparation	7
2.3.2	Stratigraphic Picks	8
2.3.3	Maps and Cross-Sections	9
3.0	Regional Geology and Hydrogeology	10
3.1	Geologic Setting	10
3.1.1	Bedrock Geology	11
3.1.2	Empress Group	13
3.1.3	Quaternary Geology	14
3.2	Hydrostratigraphy	15
3.2.1	Pierre Aquitard	15
3.2.2	Eastend-Ravenscrag Aquifer	15
3.1.3	Empress Group Aquifers	15
3.2.4	Drift Aquitard	16
3.3	Groundwater Flow	17
3.4	Groundwater Quality	19
4.0	Groundwater Model	22
4.1	Grid Discretization and Model Domain	22
4.2	Boundary Conditions	24
4.2.1	Simulation of Rivers	25
4.2.2	Constant Head	25
4.2.3	General Head	26
4.2.4	Inferred Hydraulic Discontinuities	27
4.2.5	Initial Conditions and Parameters	27
4.3	Simulation Runs	28
4.4	Calibration	29
4.4.1	Steady-State Results	30
4.4.2	Transient Results	32
4.4.3	Calibrated Parameters	35
4.5	Mass Balance	36
4.5.1	Steady-state	36
4.5.2	Transient state	37
4.6	Sensitivity Analysis	37
4.7	Validation	39
4.7.1	1965-1966 Midale Flowing Shothole	40

4.7.2	1984 Pumping Test	40
4.8	Implications on Conceptual Model	42
4.9	Predictive Simulations and Aquifer Yield	44
5.0	Summary	48
5.1.1	Recommendations	49
6.0	References	50
Appendix A: Geologic Maps and Cross-Sections		56
Appendix B: Hydrographs of Calibrated Model		57
Appendix C: Sensitivity Analysis		58
Appendix D: Hydrographs of 1984 Pumping Test		59
Appendix E: Simulated Drawdown for Various Transient Scenarios		60

List of Tables

Table 1: Historical Yields, Parameters, and Methods	5
Table 2: Concentrations of Major Ions in the Monitoring Well Network of EVA	20
Table 3: Maximum drawdown in Eastend-Ravenscrag Monitoring Wells after Five (5) Years of Pumping (Maathuis and van der Kamp, 1998)	26
Table 4: Parameters of Barrier Walls	27
Table 5: Initial Parameters	28
Table 6: Steady-State Calibration Data	31
Table 7: Statistics Measures of Transient Calibration	33
Table 8: Comparison of Observed and Modelled Drawdowns Assuming Average Pumping Rate	35
Table 9: Calibrated Parameters (changes highlighted in red)	36
Table 10: Mass Balance of the Calibrated Model at the End of Pumping Period	37
Table 11: Ranges of Acceptable Parameters Obtained via Sensitivity Analysis	38
Table 12: List of Monitoring Wells and Drawdowns During 1984 Pumping Test	41
Table 13: Available Drawdown in the Production Wells	45
Table 14: Pumping Scenarios Using Four Existing Production Wells	46

List of Figures

Figure 1: Study Area and Model Domain	6
Figure 2: Locations of SaskPower's Pumping and Observation Wells	7
Figure 3: Stratigraphic Chart in the Model Area (modified from MDH, 2010)	10
Figure 4: Bedrock Geology (modified from Simpson, 1993)	11
Figure 5: Bedrock Structure	12
Figure 6: Isopach of Eastend-Ravenscrag Formations	12
Figure 7: Outline of Empress Group and its Isopach in Major Channels	13
Figure 8: Isopach of Glacial Drift	14
Figure 9: Schematic Diagram of Distribution of Pre-Development Hydraulic Heads and Inferred Groundwater Flow in the EVA	17
Figure 10: Schematic Diagram of Regional Groundwater Flow (Meneley, 1983)	18
Figure 11: Piper Plot of Selected Chemistry Analyses	21
Figure 12: Type Log of Well PW4UL-84 Illustrating the Basis for Numerical Model	23
Figure 13: Model Boundary Conditions	25
Figure 14: Steady-State Calibration Plot	31
Figure 15: Steady-State Hydraulic Heads in the EVA (Layer 4)	31
Figure 16: Distribution of Steady-State Residual Errors in the EVA (Layer 4)	32
Figure 17: Hydrographs and Drawdowns of Wells WSA ESTEVAN and WSA OUTRAM	34
Figure 18: Average Errors per Time Step of Transient Simulation	35
Figure 19: Range of Acceptable Parameter Values Within 10% NRMS Error	39
Figure 20: Modelled and Observed Drawdowns at SRC1U-61 and WSA OUTRAM Observation Well in Response to Flowing Shothole at NE16-28-004-12W2	40
Figure 21: Distance-Drawdown Plot of the Observed and Modelled Maximum Drawdowns During the 1984 Pumping Test of PW4UL-84	42
Figure 22: Simulated Response of Monitoring Wells due to Alternative Transient Scenario	43
Figure 23: Distribution of Steady-State Drawdowns While Pumping at Rate of 1,800 dam ³ /year	46
Figure 24: Simulated Drawdowns at the Centre of SaskPower's Wells Field Using AverageRate of 4,143 dam ³ /year.	47

1.0 Introduction

Most of southeastern Saskatchewan lies within the semi-arid zone of the Canadian Prairies. Given the dry climate of the area, groundwater has played an important role in this region's development and has been used for domestic and municipal purposes, agricultural activities, and industrial purposes. The three major aquifers in southeastern Saskatchewan that could potentially support large scale withdrawals are the Estevan Valley (EVA), Tableland (TA), and Hitchcock aquifers. The most significant withdrawals from these aquifers occurred between 1988 and 1994 by SaskPower Corporation. A total of $21,339 \text{ dam}^3$ was pumped from the EVA at an average rate of $4,143 \text{ dam}^3/\text{year}$ and $18,230 \text{ dam}^3$ was pumped from the TA at an average rate of $4,080 \text{ dam}^3/\text{year}$. The water was used to supplement surface water in the Boundary Dam reservoir for cooling of two major coal-fired power generating facilities near the City of Estevan. While the pumping rates for both aquifers were seen as sustainable at the time of withdrawals, subsequent recovery/monitoring data have shown that the sustainable rate of EVA has been over-estimated in previous studies (Maathuis and van der Kamp, 1998). SaskPower does not currently use groundwater for cooling purposes. However, given the potential for increasing economic activity in the area, groundwater may be required as a water source for other industrial purposes. Additionally, in a drought event, groundwater is an attractive alternative to the growing water demands in the area.

Estimates of the sustainable yields are usually based on field methods such as long-term pumping tests and their analysis. However, pumping tests are not able to stress the aquifer for sufficient duration to provide long-term sustainable yield estimates in the buried valley aquifers. Numerical groundwater models can provide drawdown scenarios from pumping at a regional scale. To date, there have been four numerical groundwater models constructed for the EVA between 1964 and 2002 all of which appear to have over-estimated sustainable yield (Walton, 1965; Puodziunas, 1977; Van der Kamp, 1985; and Lu and Jin, 2002). These models consisted of coarse grids, simplified geology, and had variable calibration results (if any). This project aims to develop an updated numerical model to assist Water Security Agency (WSA) staff in assessing the availability of groundwater resources in the EVA and predict groundwater response from various pumping scenarios. This study will assist in the management of the groundwater resources in southeast Saskatchewan.

This work focused entirely on the EVA given its unique response (van der Kamp and Maathuis, 2012). The EVA is a deep paleo-valley filled with permeable sediments (sand and gravel) at a depth of 50 to 150 meters below ground surface. It is a long and narrow strip aquifer overlain by a low permeability aquitard and incised into a bedrock aquifer/aquitard system along its sides and below. The hydraulic response of strip aquifers to stress is different from the typical response of sheet aquifers (van der Kamp and Maathuis, 2012; Neville and van der Kamp, 2012). When stressed, strip aquifers can have large drawdowns and much larger extent of the drawdown cone than sheet aquifers. In the case of the EVA, the drawdowns are known to have extended for over 50 km along the aquifer and extended into the United States (Maathuis and van der Kamp, 1998). The risks associated with the high demand of groundwater from the EVA are the unsustainable use and potential groundwater depletion. It is important to understand the aquifer characteristics and response of these aquifers and have the ability to assess cumulative impacts of potential withdrawals to manage the limited and valuable local groundwater resource.

1.1 Historical Investigations

Speculations on pre-glacial drainage of the Missouri and Yellowstone Rivers through southeastern Saskatchewan existed as early as 1912 (Beekly, 1912, p. 323). The Geological Survey of Canada (GSC) completed a survey of the groundwater resources in southeastern Saskatchewan in 1935. This survey resulted in a series of water supply papers providing basic information on the water wells at that time and identified each well's stratigraphic production interval (i.e. bedrock or glacial). Meneley et al. (1957) were first to map the trend of buried pre-glacial channels using records collected by GSC in 1935. Christiansen and Parizek (1961) proposed a geologic model for the deposition of the valley fill deposits and began to examine the productive capacity of the aquifer.

Estimates of the safe yield of the EVA throughout the years of study have varied between 20,000 and 2,400 dam³/year (Table 1). The decrease of the estimated yield over the years of research was based on improved knowledge of the aquifer. The first safe yield estimated by Walton (1965) was 16,593 dam³/year (10 million IGPD). The study included test drilling, well construction, aquifer mapping, step test, 8-day pumping test, and aquifer analysis. The yield value was obtained using an electric analog model of groundwater flow utilizing 17,000 resistors and capacitors and simulating 12 closely-spaced production wells. Development of the numerical model included three layers, in ascending order: 1) the EVA, 2) the overlying aquitard, and 3) the upper drift aquifer (at the water table). Lateral recharge from the Eastend-Ravenscrag formations was also included. The model predicted drawdowns of up to 91 m (300 ft) around 12 theoretical production wells and up to 30 m (100 ft) at a distance of up to 16 km (10 miles) with the total affected distance ranging from 40 to 128 km away from the production wells. The model also predicted drawdown of up to 20 m (70 ft) in the upper aquifer (water table) but almost no drawdown (< 1m) in the EVA at the international border. Walton's model was not calibrated due to lack of long-term withdrawal and water level data.

Meneley (1972) suggested that the safe yield could be 13,568 dam³/year. Estimation of this yield was based on the overall recharge of the aquifer through leakage across the overlying aquitard. Puodziunas (1977) estimated an even higher yield of 20,891 dam³/year by *“modeling the aquifer as a rectangular strip aquifer 10,000 ft wide, 100 mi long and confined by 300 ft of till”* and using a development scheme of 15 wells spread evenly along the entire aquifer. He predicted a maximum drawdown of 23 m (75 ft) in the EVA and *“significant declines in the drift overlying the aquifer.”*

In 1984, Beckie Hydrogeologists Ltd (BHL) completed a major groundwater exploration program on behalf of SaskPower consisting of 27 test holes, 10 observation wells, a 29-day long pumping test, aquifer analysis, and mapping. Beckie and Pasloske (1985) estimated safe yield of at least 11,928 dam³/year and drawdowns of up to 40 m and similar extents as in Walton's (1965) model. Drawdowns were calculated at several points along the aquifer using an analytical solution, plotted on a map, and contoured. This solution assumed uniform properties, thickness, and width of the aquifer. Beckie and Pasloske (1985) recognized the limitations of such “model” and revised the initial estimates to 5,250 dam³/year based entirely on assumed 5% recharge rate from precipitation.

van der Kamp and Schneider (1983) constructed a finite-element model of the EVA. The aquifer was modelled as a single layer receiving recharge from the overlying aquitard and adjacent Ravenscrag Formation. However, this model could not be reliably calibrated due to lack of long-term production and monitoring data. Calibration of the model became possible with the additional geological and hydrogeological information collected from 1984 exploration program (Beckie and Pasloske, 1984). Using aquifer parameters from Beckie and Pasloske (1984) and van der Kamp and Schneider (1983), the model was calibrated and the safe yield estimated at 3,800–8,400 dam³/year (van der Kamp, 1985). The finite-element model was calibrated to the 29-day pumping test conducted in 1984 and the subsequent 10 months of slow recovery, which effectively extended the duration of the pumping test to 319 days (Neville and van der Kamp, 2012). The predictions of the modelled drawdowns were 40 m at the international border to 70 m at the production wells. However, it was noted that the lack of knowledge regarding the hydraulic continuity of the aquifer remained a major uncertainty.

The works of van der Kamp and Schneider (1983) and van der Kamp (1985) represent a landmark shift in understanding of the hydraulics of the EVA. The authors recognized that the previous values of safe yield were over-estimated primarily due to one major factor – aquitard leakage coefficient (or conductance). Their model demonstrated that the main controlling factor on the yield estimate is the vertical hydraulic conductivity of the overlying aquitard (K'_v) and that it is actually at least ten (10) times lower than previously thought (Walton, 1965) (Table 1). This was later confirmed by van der Kamp et. al. (1986) in their investigations of the bulk permeability of thick till overlying the Weyburn Valley Aquifer.

The lower values of leakage from the overlying aquifer resulted in reduced yield of the EVA and longer drawdown stabilization and recovery times. This lack of drawdown stabilization and incomplete recovery was evident from the 29-day pumping test, followed by 290 days of recovery monitoring. The model (van der Kamp, 1985) suggested that drawdowns would stabilize after 5 – 10 years of pumping, depending on the pumping rate. Given the lower K'_v of the aquitard, van der Kamp (1985) also concluded that production from the EVA was unlikely to affect the water table or surface water bodies.

Maathuis and van der Kamp (1989) used data from 257 days of production in 1988-1989 and the previously built model (van der Kamp, 1985) to suggest that a yield of 4,500 dam³/year was sustainable in the long-term. The feasibility of higher production rates could not be assessed due to an insufficient recovery period. The drawdowns during this production period reached 30 m at the pumping wells and less than 5 m at the international border. The drawdowns modelled by van der Kamp (1985) were in good agreement with the observed drawdowns for the pumping period, at least in the short-term. This model was then used to predict the impact after 10 years of pumping at a rate of 4,500 dam³/year and showed that the drawdowns would stabilize at 50 m at the production wells and 25 m at the international border. The extended production period also revealed the presence of complete blockage in the Missouri Channel and partial blockage of the EVA northeast of the production wells.

A total volume of 21,339 dam³ was withdrawn from the EVA between September 1988 and May 1994. Van Stempvoort and Simpson (1994) reviewed the aquifer response to the 5-year pumping period and re-assessed the sustainable yield to be ~ 4,000 dam³/year, which coincided with the average production rate over the entire 5-year period. This yield was based entirely on qualitative review of response to pumping at several monitoring wells, which apparently showed stabilization of drawdowns. However, it was subsequently found that the water levels did not stabilize. In addition, the report produced several computer-generated maps of the EVA and associated surfaces as well as a stratigraphic database. This stratigraphic database was based on earlier mapping of southeastern Saskatchewan done by Simpson (1993).

Maathuis and van der Kamp (1998) undertook a detailed review of the five (5) years of pumping and the four (4) years of recovery data existing at that time. Hydrographs of all monitoring wells were evaluated both qualitatively and quantitatively. Quantitative analysis of the drawdown and recovery was based on linear systems analysis. This technique uses calculated constant-rate drawdown curves to predict aquifer behavior (van der Kamp, 1989). They obtained constants for an exponential function that was in good agreement with the observed data and then used this equation to predict recovery. Using best-fit functions for selected monitoring locations, Maathuis and van der Kamp (1998) showed that drawdowns did not stabilize after five (5) years of pumping as suggested by van Stempvoort and Simpson (1994), but would have increased by another 25 – 36% if pumping continued at the previous rate. Since the drawdowns are directly proportional to pumping rates, the estimated sustainable yield was reduced to 2,400 – 2,800 dam³/year. Moreover, they predicted that drawdown stabilization would occur over at least a 20-year period, much longer than previously thought.

Lu and Jin (2002) developed a finite-difference model (MODFLOW) of the EVA utilizing aquifer maps from van Stempvoort and Simpson (1994) and using input aquifer properties from van der Kamp (1985). The estimated safe yield from the model was up to **6,200 dam³/year** at steady-state. Similar to previous models, this model consisted of three layers, in ascending order: 1) underlying aquitard, 2) the EVA (single layer), and 3) the overlying aquitard. The MODFLOW model was calibrated using five (5) years of production and four (4) years of recovery data. The calibration results ranged from 1 to 13.5 m of head difference between the measured and modelled levels. Similar to previous models, the sensitivity analysis has shown that the MODFLOW model was most sensitive to changes in the vertical hydraulic conductivity (K'_v) of overlying aquitard.

Table 1: Historical Yields, Parameters, and Methods

Authors	Yield (dam ³ /year)	Basis for Yield Estimate	EVA			Overlying Aquitard			Aquifer Test Data Used
			T (m ² /d)	S	b (m)	K _v ' (m/s)	b' (m)	L (s ⁻¹)	
Walton (1965)	16,593	Electric analog model	746-5966	2.2×10 ⁻⁴	7.62	5.7×10 ⁻⁹	60 - 91	7.4×10 ⁻¹⁰ 5.4×10 ⁻¹¹	8 days pumping No recovery data
Meneley (1972)	13,568	Unknown							
Puodziunas (1977)	20,891	Model (details unknown)	1863				91		
Beckie and Pasloske (1985)	> 11,928	Analytical model	2043-2103	3.0×10 ⁻⁴		5.7×10 ⁻⁹	50 - 76	1.1×10 ⁻¹⁰ 7.4×10 ⁻¹¹	29 days pumping 290 days recovery
Beckie and Pasloske (1985)	5,250	Recharge (5% of precipitation)							
Van der Kamp (1985)	3,800-8,400	Finite-element model	720	2.4×10 ⁻⁴	40 - 100	3.2×10 ⁻¹⁰	80	4.0×10 ⁻¹²	29 days pumping 290 days recovery
Maathuis and van der Kamp (1989)	>4,500	Production history and 1985 model							257 days pumping
Van Stempvoort and Simpson (1994)	4,000	Production history							5+ years pumping
Maathuis and van der Kamp (1998)	2,400-2,800	Drawdown and recovery model	720-860	2.4×10 ⁻⁴ 8.0×10 ⁻⁴	< 80	3.2×10 ⁻¹⁰ 8.3×10 ⁻¹⁰	50 - 100	6.4×10 ⁻¹² 8.3×10 ⁻¹²	5+ years pumping 4 years recovery
Lu and Jin (2002)	< 6,200	Finite-difference model (ModFlow)	242-1037	6.0×10 ⁻⁵	40	2.7×10 ⁻¹⁰	60	5.0×10 ⁻¹²	5+ years pumping 4 years recovery

T = Transmissivity of EVA

S = Storativity of EVA

b = Thickness of EVA

K_v' = Vertical hydraulic conductivity of overlying aquitard

b' = Thickness of overlying aquitard

L = Leakage coefficient of overlying aquitard

2.0 Data and Methods

2.1 Study Area

This study focused on the Estevan Valley Aquifer (EVA). The spatial extent and distribution of the aquifer includes the area between townships 01-06, range 01-20, West of the 2nd meridian (Figure 1). The model domain was reduced to townships 01-05 and ranges 04-13 to reflect model's boundary conditions. This area was chosen based on current geological and hydrogeological information that was incorporated into the model since 1994 (van Stempvoort and Simpson, 1994).

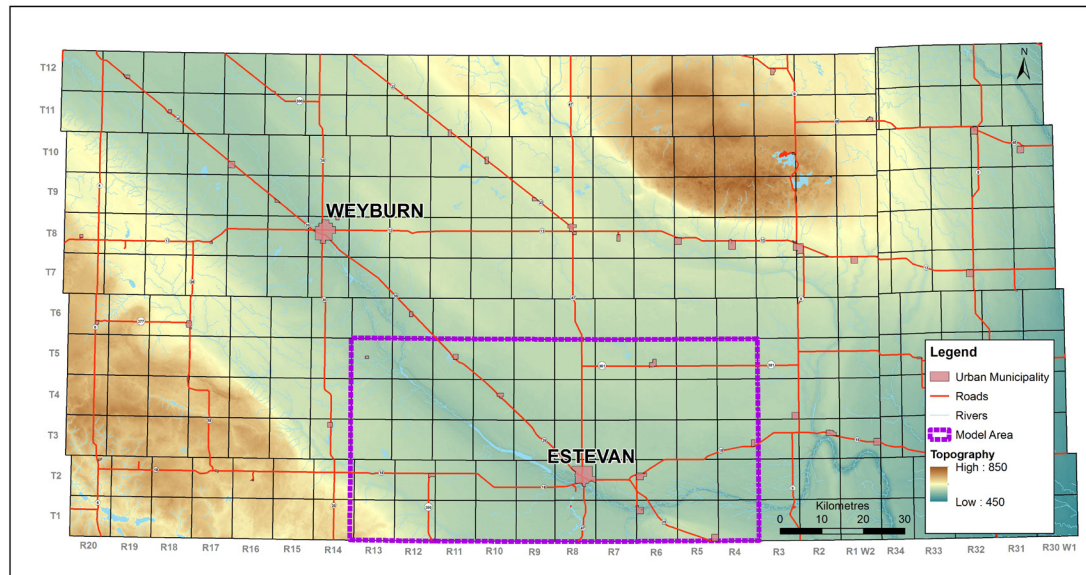


Figure 1: Study Area and Model Domain

2.2 Geological and Hydrogeological Information

Information from the van Stempvoort and Simpson (1994) report formed the foundation of this work. These data were extracted from the database found on the six floppy disks in Appendix C – E of van Stempvoort and Simpson (1994) report. These data include groundwater pumping records, WSA water well database (current to 1992), SaskPower's monitoring wells (Figure 2) and water levels (up to 1994), stratigraphic picks, static water levels, and groundwater quality database.

Additional water level data from monitoring wells were obtained from SaskPower's monitoring reports for years 1995-1996. These reports contained additional two years of recovery data after cessation of pumping. Recovery data from SaskPower's monitoring wells were collected by the Saskatchewan Research Council (SRC) until 2010 and were included in model development. Additional recovery data up to year 2015 were obtained from two provincial observation wells, WSA Estevan and WSA Outram.

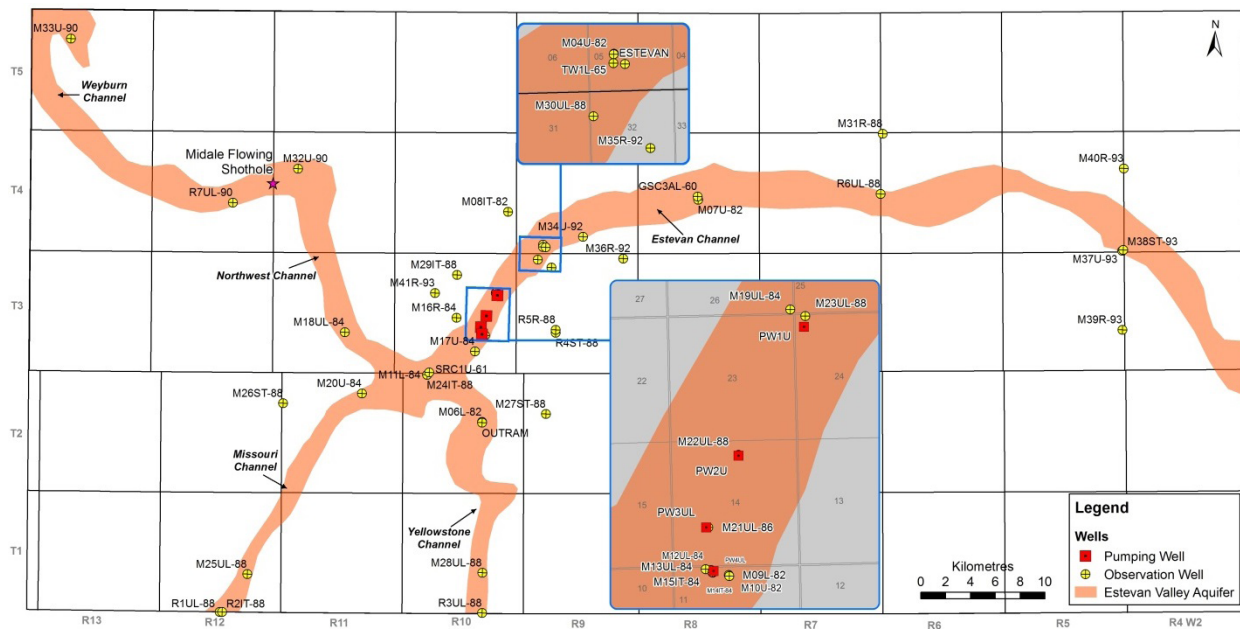


Figure 2: Locations of SaskPower's Pumping and Observation Wells

The water well database used for stratigraphic picks in the van Stempvoort and Simpson (1994) report are current up to year 1992. Numerous wells have been completed since 1992 and incorporation of updated information was required. Therefore, WSA's water well database was queried and all wells between Township 1 – 12 and Range 30W1 – 20W2 drilled up to the year of 2014 were extracted. Well information and lithology data were assessed, evaluated for incorporation into the model.

2.3 Data Processing

2.3.1 Data Preparation

A review of WSA's Water Well Drillers Report database was completed in order to identify any new wells suitable to be added into the geologic database. First, wells in the existing 1995 database were cross-referenced to the WSA's water well database in order to avoid duplication of wells. Each well record in SRC's database was identified by a unique "acquisition number." Every well with an acquisition number was cross-referenced to the corresponding WWDR number in the WSA database by manually examining well records. The SRC database contained borehole information, such as coal and hydrocarbon exploration logs, that was not in the WSA database.

The second step involved mapping of SRC-picked wells and all other wells from WSA database. While the matched SRC wells contain UTM coordinate system in NAD27 datum, the locations of the wells from the WSA database are described by the Legal Land Description (LSD). The LSDs were converted to UTM coordinate system based on the centroid of the quarter section in NAD 83, extended zone 13 datum. Having obtained coordinates, all wells were plotted on a map.

The third step involved identification of wells that are to be added to the final database. This step was necessary to ensure that only wells that were completed in the EVA and into the bedrock formation, containing relevant/useful information, were added to the database. This required manual examination of all wells that have not been included in SRC's mapping (both pre- and post-1992), as shown on the post map created in the second step. Once identified, the additional wells (header and lithology) were added to the database. Each well record is clearly identified as new and whether it has E-log and/or lithologic description. Data from the SRC (van Stempvoort and Simpson, 1994) were treated as the highest quality because they were already interpreted and verified by a professional geoscientist. The second highest quality data consisted of new wells that included both an E-log and lithologic description – these wells were added to the database automatically. The lower quality data consisted of wells with only lithologic descriptions (driller's log). These wells had to be of sufficient depth to be included in the database. For example, a well that appears to have intersected sand and gravel of the Empress Group (based on the depth from SRC maps) but has not necessarily reached bedrock surface would be included in the database. At a minimum, such a well would indicate the likely presence of a channel and possibly Empress Group. For example, well #113480 at location NW-03-04-09W2 suggests the presence of a potential channel to a depth of at least 420 feet.

Previous mapping by SRC utilized only the highest quality data – wells with good quality E-logs and a lithologic description. This approach is acceptable when there are time constraints and mapping is done on a regional scale. However, lack of any consideration of lower quality data can lead to oversimplified interpretation and missed/by-passed local geologic features. This is especially true in areas with very little data or with narrow geologic features such as channels.

Low quality data in the context of this work consist of driller's lithologic descriptions without E-logs. These descriptions can be inconsistent between different water well drillers. Nevertheless, for most wells, drillers provide the only available account of the sediment and these records should not be automatically discarded. Therefore, these data should be looked at (minimum) and used with caution when possible. Note that these lower quality data can be easily identified and removed from the database later, if such decision is made.

2.3.2 Stratigraphic Picks

Stratigraphic picks from wells examined by SRC (van Stempvoort and Simpson, 1994) were automatically considered of highest quality, and in fact, were cross-referenced in order to maintain consistency with the picks in the newly added wells. Formation tops were assigned to all new wells based on E-logs (where available) and/or lithology descriptions. For the most part, lithologic descriptions appeared consistent with the E-logs. Wells without E-logs were picked with caution recognizing that the lithologic description may be inconsistent. Wells with poor descriptions or descriptions that appear to conflict with the interpreted regional geology were removed from the database. In general, data quality control is a dynamic process with records being added and deleted continuously based on the understanding of the characteristics of the buried valley aquifer.

Identification of stratigraphic units was done manually on a well-by-well basis. Following the phased approach to separation of stratigraphic units described by Schreiner (2010), only Phase 1 stratigraphic units were identified. These units include bedrock, Empress Group, and drift. Where possible, bedrock was further subdivided into Pierre Shale and Eastend-Ravenscrag intervals. Further separation of drift deposits was not completed given the lack of carbonate data. Phase 1 stratigraphy is sufficient for the purpose of this project, which is focused on the Empress Group aquifers. It should be noted that the SRC database contains identified stratigraphy up to Phase 4 (complete Quaternary stratigraphy). A future attempt can be made to identify detailed Quaternary stratigraphy in the new wells associated with E-logs.

The elevations of the stratigraphic units in the newly added wells were determined the digital elevation model (DEM). The DEM raster dataset was obtained from the Saskatchewan Geospatial Imagery Collaborative (SGIC) group with a cell size of 15 m and stated vertical accuracy of ± 3 m at 90% confidence. Elevations were estimated from the quarter-section or LSD centroid point. It is recognized that this approach may introduce errors on the cross-sections because the elevation at the calculated centroid point is different from the actual elevation of the well.

2.3.3 Maps and Cross-Sections

The majority of the historical reports and their maps are found in hard copies. Some features had to be scanned and digitized. Maps containing valuable information were georeferenced. Features that were digitized include:

1. Most recent outlines of Empress Group and valleys.
2. Locations (coordinates) of the monitoring wells. Accurate placement of monitoring wells is important when doing any modelling work since response to pumping is highly dependent on the distance from the pumping wells.
3. Locations of inferred hydraulic discontinuities.
4. Location of nine EM lines that were used to delineate channels (Simpson, 1996; Komex, 2003).

The bedrock surface has been contoured using a combined stratigraphic picks database consisting of the SRC database and newly added wells. Prior to contouring, it was noted that the bedrock surface map from the van Stempvoort and Simpson (1994) report, Map A2, were created using computer-generated contours (Stratlog II). Review of existing geologic maps in the area showed that the second generation mapping by SRC (Simpson, 1993) provided the most reliable basis of the bedrock surface. The bedrock map was likely hand contoured with great thought put into the geologic interpretation, even in places with few data points. Therefore, this map was used as a guide to the newly contoured bedrock surface. Subsequent work by Maathuis and Simpson (2003a, 2003b) was based on the interpretation of the 1993 mapping and new data.

All wells were posted on a map and labeled with the bedrock elevation (Figure A.9). The quality of these data was clearly identified by the different symbols and wells with Empress Group (where present) were circled. The map was hand contoured using professional judgement and in accordance with previous work. Preference was given to wells interpreted by SRC and new wells with E-logs. New wells without E-logs were only consulted in areas of sparse data and with caution. The contouring interval was 20 m, which is coarse enough to mask any errors that may have resulted from incorrect surface elevations thereby minimizing the need to revisit ground elevations.

Six cross-sections of the EVA were created using the stratigraphic database, E-logs, and lithologic descriptions. Wells and testholes with E-logs, monitoring wells, and wells with professional lithologic descriptions were preferentially selected for the cross-sections. There are three transverse and three longitudinal cross-sections (Appendix A). Transverse cross-sections attempt to capture the shape of the entire channel. Longitudinal cross-sections pass through the deepest known parts of the EVA in an attempt to investigate aquifer continuity.

An attempt has been to trace sands and gravels of the Empress Group across and along the EVA. However, continuity of each individual sand/gravel interval could not be established with certainty over long distances using boreholes alone given the complexity of fluvial depositional environment.

3.0 Regional Geology and Hydrogeology

3.1 Geologic Setting

The Empress Group sediments were deposited in four interconnected paleo-channels: the Missouri, Yellowstone, Estevan, and Northwest channels and covered by glacial deposits consisting primarily of till belonging to the Sutherland and Saskatoon Groups. These channels are of pre-glacial origin and have been incised into the bedrock. The term bedrock refers to Late Cretaceous sediments of the Pierre, Eastend, Whitemud, and Frenchman Formations and the Tertiary age Ravenscrag Formation and Lower Empress (Figure 3).

TIME	STRATIGRAPHY			LITHOLOGY		SYMBOL	
PERIOD	GROUP	FORMATION	UNIT OR MEMBER				
QUATERNARY	Saskatoon	Surficial Stratified Deposits	Alluvium	Silt, Sand, Gravel	Clay, Silt, Sand	Qa ³	Qa ³
				Silt, Sand, Gravel	Clay, Silt, Sand	Qa ²	Qa ²
		Haultain		Silt, Sand, Gravel	Clay, Silt, Sand	Qh ³	Qh ³
				Silt, Sand, Gravel	Clay, Silt, Sand	Qh ⁴	Qh ⁴
		Battleford		Till		Qb-ut	
				Gravel, Sand, Silt, Clay		Qb-s	Qb
				Till		Qb-lt	
		Floral	Upper	Till		Qf-ut	
			Riddell (Middle)	Gravel, Sand		Qf-ms	
			Lower	Till		Qf-lt	Qf
				Gravel, Sand, Silt, Clay		Qf-ls	
				Till		Qf-bt	
	Sutherland	Warman		Till		Qw-t	Qw
				Gravel, Sand, Silt, Clay		Qw-s	
		Dundum	Upper	Till		Qd-ut	
				Gravel, Sand, Silt, Clay		Qd-us	
			Lower	Till		Qd-lt	Qd
				Gravel, Sand, Silt, Clay		Qd-ls	
		Mennon	Upper	Till		Qm-ut	
				Gravel, Sand, Silt, Clay		Qm-s	Qm
			Lower	Till		Qm-lt	
	Empress		Upper	Gravel, Sand, Silt, Clay (Proglacial)		Qe	QTe
			Lower	Chert and Quartzite Sand on Gravel (Preglacial)		Te	
TERTIARY	Ravenscrag			Sand, Clay, Silt, Sandstone, Siltstone, Mudstone		Tr ¹²	
			Short Creek Zone	Lignite Seams		Trsc	
				Sand, Clay, Silt, Sandstone, Siltstone, Mudstone		Tr ¹¹	
			Roche Percee Zone	Lignite Seams		Trrp	
				Sand, Clay, Silt, Sandstone, Siltstone, Mudstone		Tr ¹⁰	
			Souris Zone	Lignite Seams		Trs	Tr
				Sand, Clay, Silt, Sandstone, Siltstone, Mudstone		Tr ⁹	
			Estevan Zone	Lignite Seams		Tre	
				Sand, Clay, Silt, Sandstone, Siltstone, Mudstone		Tr ⁸	
			Boundary Zone	Lignite Seams		Trb	
CRETACEOUS	Montana	Frenchman		Sand and Silt		Kf	
			Whitemud	Sand and Clay		Kw	Kfwe
		Eastend		Sand and Silt		Ke	
		Pierre		Silt and Clay		Kp	

Figure 3: Stratigraphic Chart in the Model Area (modified from MDH, 2010)

3.1.1 Bedrock Geology

The oldest sediments subcropping in the study area belong to the Pierre Formation, which is composed of soft, grey, non-calcareous, marine, silt and clay. Overlying the Pierre Formation (in ascending order) are the Eastend, Whitemud, Frenchman, and Ravenscrag formations. The Eastend Formation is composed of grey or green sand, silt, and clay with thin coal seams in the upper part (Figure 3). The Whitemud Formation is composed of kaolinized, white sand and clay and the Frenchman Formation is composed of sand, silt, and clay with local bentonite and calcareous zones. The uppermost bedrock consists of the Ravenscrag Formation. The Ravenscrag Formation is composed of coal-bearing sand, silt and clay. In the absence of coal, the Ravenscrag Formation is indistinguishable from Frenchman and Eastend and is often referred to as Eastend-Ravenscrag interval.

The bedrock surface was shaped by a combination of pre-glacial, pro-glacial, and glacial erosion. The bedrock surface in the southern parts of the study area consists of Ravenscrag Formation transitioning to Pierre Shale in the north (Figure 4). The topography of the bedrock is influenced by erosional channels of northward flowing pre-glacial Missouri and Yellowstone rivers. These rivers merged north of Township 2 into a single channel forming the main body of the Estevan Valley. The Northwest channel may have also contributed flow into the Estevan Valley; however, the timing of that contribution is unclear (pre-glacial or post-glacial).

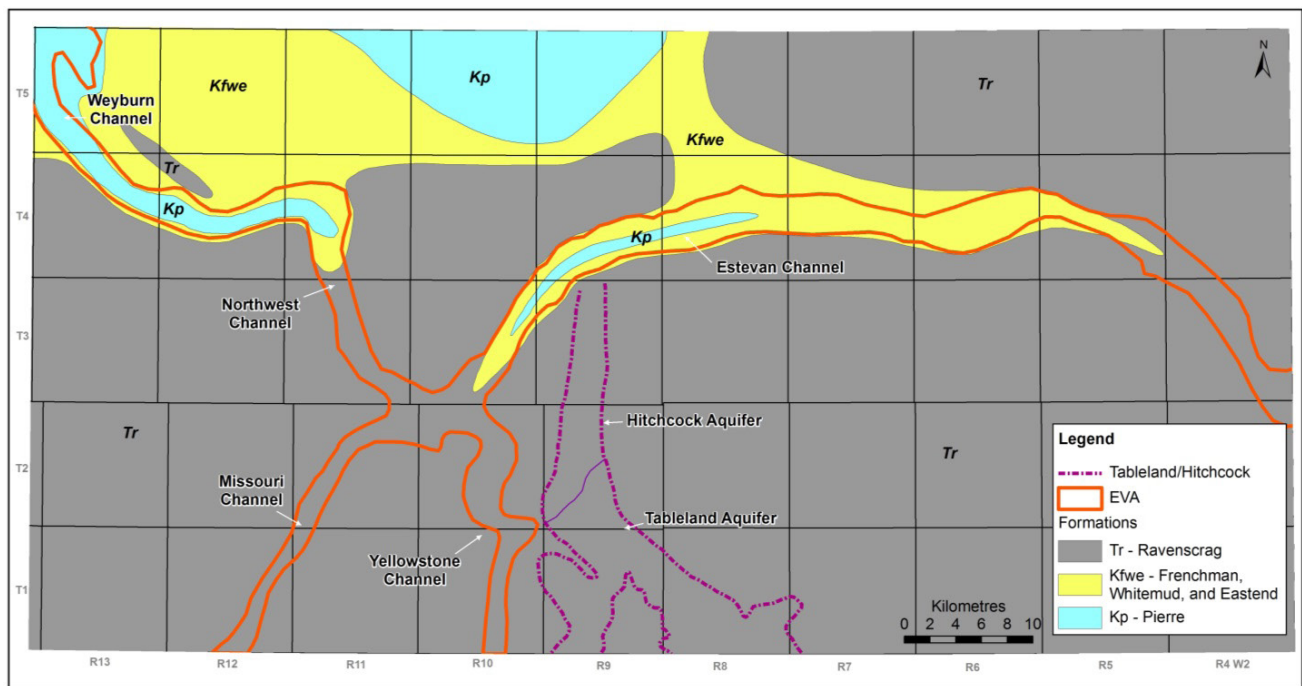


Figure 4: Bedrock Geology (modified from Simpson, 1993)

The bedrock elevation ranges from < 400 metres above sea level (masl) in the eroded valleys in the southeast portion of the study area to > 650 masl in the southwestern and northern portions of the modelled area (Figure 5). The elevation change within the paleo-valleys is from 450-460 masl at the international border in the Missouri and Yellowstone channels to 400 masl in east to 450-460 masl in the eastern portion of the Estevan channel. In this project, the Eastend, Whitemud, Frenchman, and Ravenscrag Formations were mapped as a single unit due to difficulty of distinguishing between them using lithologic or geophysical logs. This amalgamated interval is referred to as Eastend-Ravenscrag Formations. Its thickest intervals of up to 320 m occur in the southeast part of the study area (Figure 6).

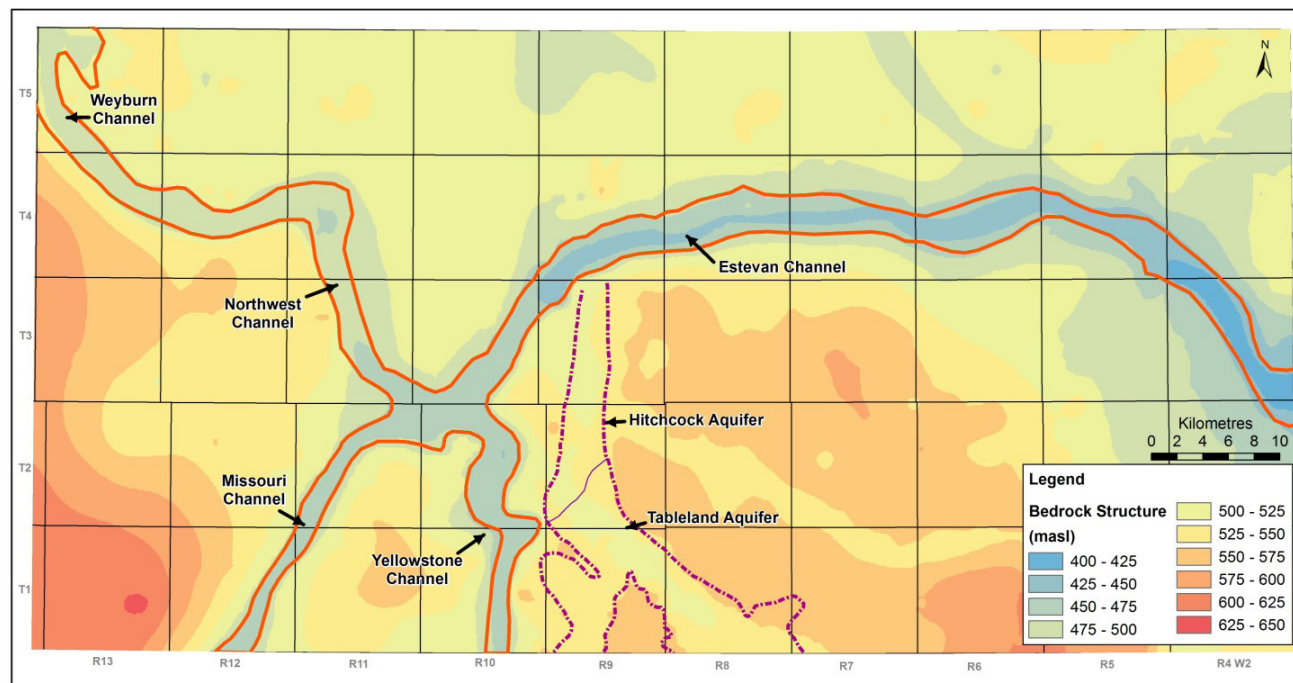


Figure 5: Bedrock Structure

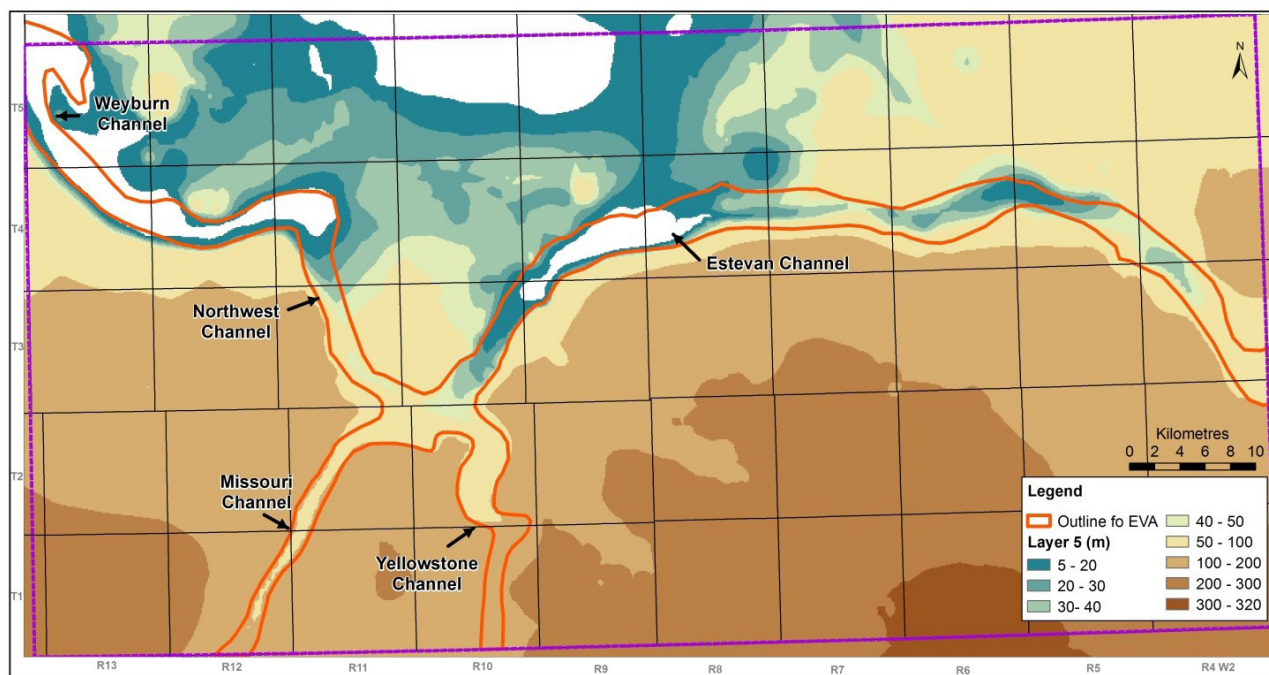


Figure 6: Isopach of Eastend-Ravenscrag Formations

3.1.2 Empress Group

The Empress Group is generally defined as stratified fluvial sand, gravel, clay and silt deposits between the underlying bedrock and the overlying till (Whitaker and Christiansen, 1972). These deposits tend to occupy pre-glacial and pro-glacial valleys incised into the bedrock but may also occur in the uplands. The total thickness of Empress Group (Figure 7) is up to 80 m with the top elevation of up to 510 masl at the SaskPower's production well sites (TWP 03, RG 10W2). The top elevation of Empress Group gradually decreases to < 480 masl approximately 30 km further to the east from the production wells along the channel (Figures A.10-A.15).

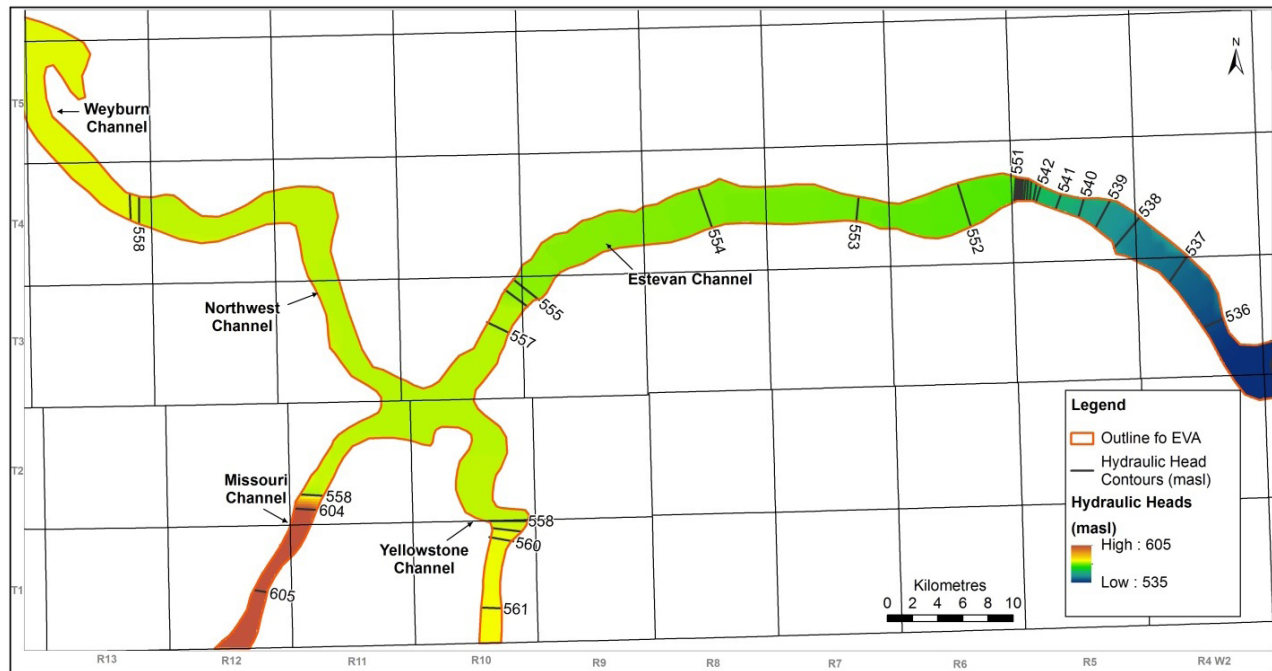


Figure 7: Outline of Empress Group and its Isopach in Major Channels

The lower or the basal gravels of the Empress Group are commonly composed of chert and quartzite pebbles and cobbles, interbedded with sand grains of similar composition. These sediments are often described as brown sands and gravels. The lower deposits are commonly non-calcareous which suggests (along with quartzite and chert) that they are of pre-glacial origin (Late Tertiary age) sourced from the west and southwest.

The basal contact of the Empress Group is very distinct both on E-logs and in lithologic description. Where the Empress Group overlies the Pierre Formation, the unconformity is characterized by the underlying compact, grey, non-calcareous clay or silt of the Pierre Formation overlain by gravel, sand, or soft calcareous silt or clay of the Empress Group. Where the bedrock consists of Eastend–Ravenscrag Formations, the unconformity is characterized by the bedrock surface consisting of non-calcareous, bedrock sands, silts, and clays with abundant coal fragments and the overlying gravels, sands, or silts of the Empress Group (Christiansen, 1983).

Sands and gravels of the upper part of the Empress Group can be composed of igneous, metamorphic, and carbonate clasts with lesser amounts of chert and quartzite (Whitaker and Christiansen, 1972). The upper sands and gravels are calcareous, which suggests that they are of glacial origin (Quaternary age) whereby glaciers brought igneous, metamorphic, and carbonate sediments from the northeast. The upper boundary of Empress Group is characterized by sands, gravels and silts below and the till above. The upper contact can be difficult to identify if the Empress Group has been subjected to erosion and the overlying deposits are composed of the stratified intertill sediments. These intertill sediments are included within Empress Group if they cannot be separated on a lithologic basis.

3.1.3 Quaternary Geology

The Quaternary deposits in the study area consist of till and stratified deposits of glacial origin, which is commonly referred to as “drift.” The drift in the study area can be up to 220 m thick with thicker portions in the incised valleys and overlying the Empress Group (Figure 8). Till is composed of unsorted mixture of gravel, sand, silt, and clay-dominated matrix deposited in place by a melting glacier. The meltwater from the ice further eroded and redeposited stratified (i.e. sorted to some degree) gravels, sands, silts, and clays from the till or fragments of bedrock. This process has likely occurred multiple times as glaciers retreated and re-advanced in the Quaternary Period. The drift has been differentiated into Sutherland and Saskatoon groups and their formations based on information such as carbonate content and electric log signatures (Christiansen, 1968). These groups can also be differentiated on the basis of weathering zones separating them signified by leaching, oxidation, staining, and other alteration features (van Stempvoort and Simpson, 1994).

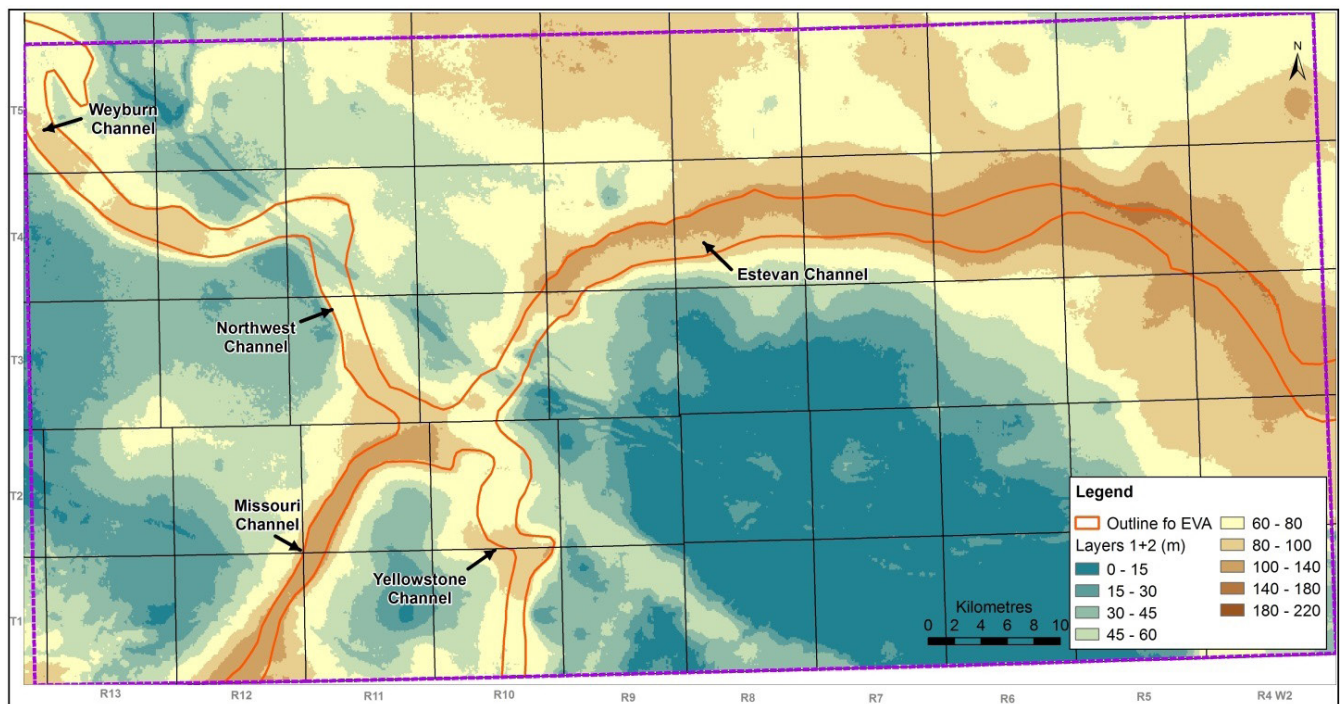


Figure 8: Isopach of Glacial Drift

The Sutherland Group overlies the Empress Group, where present, or directly on the bedrock surface. The Sutherland Group includes the Mennon, Dundurn, and Warman Formations (in ascending order). These formations are composed of variable proportions of tills and stratified deposits (Figure 3). Most of the intertill aquifers identified in the study area are contained within the upper part of Sutherland Group (van Stempvoort and Simpson, 1994).

Overlying the Sutherland Group is the Saskatoon Group, which consists of the Floral and Battleford Formations and the Surficial Stratified Deposits. The Saskatoon Group contains more sand, is more resistive, and has higher carbonate content than the underlying Sutherland Group. Surficial deposits occur as eolian, glaciolacustrine, glaciofluvial and as alluvial sediments that were deposited during and after the final deglaciation (van Stempvoort and Simpson, 1994).

SRC's geologic database (van Stempvoort and Simpson, 1994) contains geologic picks of Sutherland and Saskatoon groups and their formations; however, mapping of these geological units is yet to be completed in southeastern Saskatchewan. Therefore, this work provides only general overview of the Quaternary geology and, for the purposes of groundwater model, considers the Sutherland and Saskatoon Group as one unit – the drift.

3.2 Hydrostratigraphy

3.2.1 Pierre Aquitard

The Pierre Formation is composed of soft, grey, non-calcareous, marine clay and is regarded as an aquitard. The top of the Pierre Formation is referred to as the *base of groundwater exploration*, meaning that below the formation, groundwater supply is generally not economically feasible.

3.2.2 Eastend-Ravenscrag Aquifer

The Eastend-Whitemud, Frenchman, and Ravenscrag Formations were amalgamated into a single hydrostratigraphic unit referred to as Eastend-Ravenscrag Formations. Where the Eastend-Ravenscrag Formations are saturated, they form a complex bedrock aquifer system. The Ravenscrag-Eastend Aquifer (also known as the Bienfait Aquifer, Meneley, 1983) is absent due to erosion in areas to the north of and within the paleo-channels (Figure 6). The thickest intervals of up to 320 m occur in the southeast part of the study area. The aquifer outcrops in the southeast part of the study area and along some parts of the Souris River valley.

3.1.3 Empress Group Aquifers

The largest Empress Group aquifers in southeast Saskatchewan are the Estevan Valley, Tableland, and Hitchcock aquifers (Figure 5). It is a complex aquifer system consisting of multiple interconnected layers of sand and gravel extending south into North Dakota. Regionally, the aquifers are incised into the Ravenscrag Formation; however, it may be bounded by the Eastend-Frenchman and Pierre Formations at the local scale.

The lower sediments of the Empress Group within Northwest, Missouri, Yellowstone, and Estevan Channels form the EVA. The EVA is approximately 70 km long, 4 km wide and up to 40 meters thick. In the Estevan Channel, the EVA consists of two main sand and gravel intervals. The lowermost gravel interval is composed of mainly chert and quartzite. This interval is up to 10 m thick and appears to be restricted to the lowest point within the channel at elevation of < 450 masl. The upper interval is separated from the lower gravel by silt or clay and is composed of a mixture of sand and gravel of mainly granitic and igneous origin, although some chert and quartzite can also be present. This interval is found at approximate elevations of 460 – 480 masl at the production site. The intervening silty clay layer is locally absent in some wells and the two sand and gravel intervals may be directly connected.

The sediments that overlie the EVA and that by definition belong to Empress Group are termed as “Upper Empress” (Figure 12). This hydrostratigraphic unit is classified as an aquifer relative to the overlying tills. The Upper Empress appears to contain greater proportion (by thickness) of finer grained sediments (silts) than the underlying EVA. This can explain delayed and reduced response to pumping as observed in some observation wells completed in this interval (Maathuis and van der Kamp, 1998). The thickest section of Upper Empress is up to 50 m and found at the production site (TWP 03, RG 10W2). Upper Empress occupies the upper portions of the paleo-channels and thus appears to be wider (up to 4 km) than the underlying EVA. The Upper Empress is aerially less extensive than EVA, with the bulk of its sediments present in the Yellowstone and Estevan channels. Note that Beckie and Pasloske (1985) considered this unit to be an intertill aquifer; however, in this report it was classified as part of Empress Group due to absence of underlying tills and for consistent interpretation with historical terminology by Whitaker and Christiansen (1972) and geologic picks from SRC.

The Tableland Aquifer lies east of the Yellowstone channel of the Estevan Valley Aquifer and extends north from the North Dakota border to Township 2 (Figure 5). The Tableland Aquifer is defined as a buried valley incised into the Eastend-Ravenscrag Formation and subsequently filled with glacial sediments belonging to the Empress Group. Sediments consist of coarse gravel with cobbles at the bottom. In Saskatchewan, the aquifer is approximately 125 km² and up to 85 km² in the U.S. It is up to 5 km wide with an average thickness of 20 meters overlain by approximately 30 m of glacial drift (Maathuis and van der Kamp, 1998).

The northern boundary of the Tableland aquifer is marked by a hydraulic discontinuity located in the vicinity of Township 02, Range 09. van Stempvoort and Simpson (1994) named the aquifer north of the discontinuity as the Hitchcock aquifer (Figure 5). The Hitchcock aquifer consists of pre-glacial channel deposits composed of a lower and upper units. The lower unit consists of basal gravel, siltstones, and black shales and the top unit consists of gravel, sand, and silt. The aquifer is approximately 10 to 30 m thick overlain by 30 to 40 m of glacial drift.

3.2.4 Drift Aquitard

The Sutherland and Saskatoon Group sediments overlie the Empress Group aquifers. Saturated fine sands within the till form potential aquifers within the Sutherland and Saskatoon Group sediments. The aquifers are discontinuous and are variable in thickness. Differentiation between the Sutherland and Saskatoon Group aquifers has yet to be completed in southeast Saskatchewan and aquifer properties are not well understood, the two groups were considered as a single unit herein referred to as the Drift Aquitard. While it is recognized that various intra/inter-till aquifers exist within the unit, the Drift is considered to be an aquitard with respect to the underlying Empress Group. This is due to the relatively low hydraulic conductivity of tills, which comprise the bulk of Drift sediments. Drift Aquitard is thin (< 15 m) or absent between townships 1-3, ranges 5-9 or along the Souris River valley (Figure 8). Thickest sections of drift of up to 220 m are found to be overlying the paleo-channels.

3.3 Groundwater Flow

The pre-pumping static hydraulic heads in the EVA generally range between 563 masl in the Yellowstone Channel to 550 masl in the Estevan Channel over a distance of 70 + km (Figure 9). Hydraulic heads gradually decrease to 535 masl east of Range 4. Hydraulic heads in the Missouri channel are 603 – 604 masl and at least 40 m higher than the rest of the adjacent aquifer due to hydraulic discontinuity separating the Missouri Channel from the rest of the aquifer. The hydraulic gradients at the confluence of channels and SaskPower’s well field are very low (10^{-6} – 10^{-5} m/m) and increase in the Yellowstone and Estevan Channels (10^{-5} – 10^{-3} m/m) due to greater variations in aquifer properties or presence of hydraulic discontinuities. In general, the EVA appears to be hydraulically continuous throughout its central parts (i.e. confluence of channels) as indicated by the low hydraulic gradient and pumping tests (Walton, 1965; Beckie and Pasloske, 1985). These pumping tests have also yielded hydraulic conductivity values between 10^{-4} – 10^{-3} m/s.

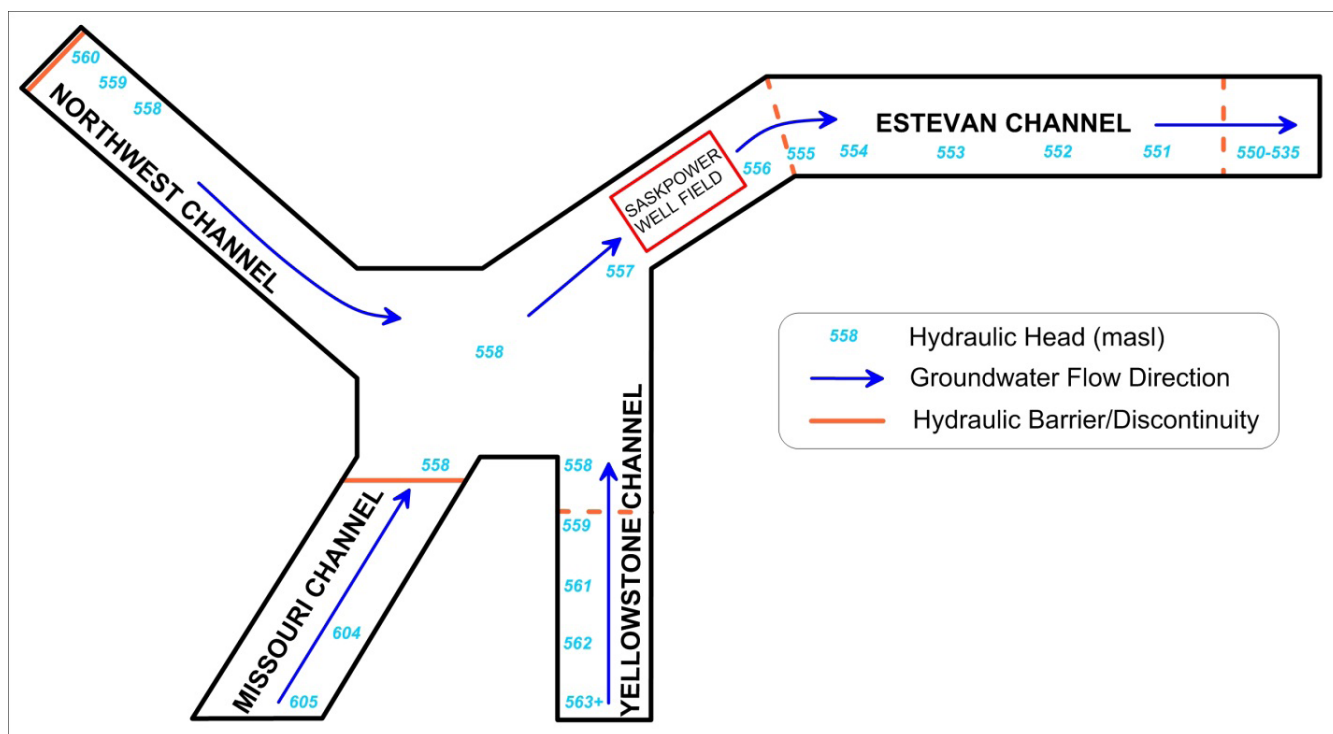


Figure 9: Schematic Diagram of Distribution of Pre-Development Hydraulic Heads and Inferred Groundwater Flow in the EVA

Several inferred hydraulic discontinuities or “barriers” cut across the EVA (Figure 9). The exact nature of these discontinuities is unknown but it can be assumed they are caused by reduction in hydraulic conductivity due to lithological variations, change in aquifer thickness, or some combination of both reflecting the complex nature of the fluvial deposits. The inferred hydraulic discontinuities affect the water levels and groundwater flow ranging from slight reduction in hydraulic head to complete blockage of some parts of the aquifer. For example, the EVA in the Missouri Channel appears to be isolated from the rest of the EVA by a hydraulic discontinuity as indicated by a change in hydraulic head and no drawdowns from withdrawal. Water levels in the Missouri Channel showed negligible response during the peak of groundwater withdrawals across the hydraulic discontinuity, which resulted in drawdowns of 30 – 50 m throughout the rest of the EVA. In total, there appears to be five inferred hydraulic discontinuities: four hydraulic discontinuities were previously documented by Maathuis and van der Kamp (1998).

One additional discontinuity was applied in the Yellowstone Channel to improve calibration of this groundwater model. Note that improved calibration in the Yellowstone Channel could also be achieved by reducing hydraulic conductivity of the EVA. However, this method was avoided due to the absence of any factual aquifer properties and detailed geology in this area. Additional details regarding boundary conditions are discussed in Section 4.2.

Groundwater flow in the EVA is dominated by lateral flow along the channel. The general flow directions are from the Missouri, Yellowstone, and Northwest channels towards the Estevan Channel and then eastwards in the Estevan channel (Figure 9). Local topography appears to have low to moderate influence on the hydraulic heads suggesting the EVA is likely a part of a confined intermediate flow system. For example, high artesian heads are maintained in low-lying areas where Souris River cuts through the Drift overlying the aquifer. The potentiometric surface and high hydraulic conductivity of the EVA indicate that it functions as a regional drain of the Eastend-Ravenscrag Aquifer from the north and from south (Figure 10) (Meneley, 1983).

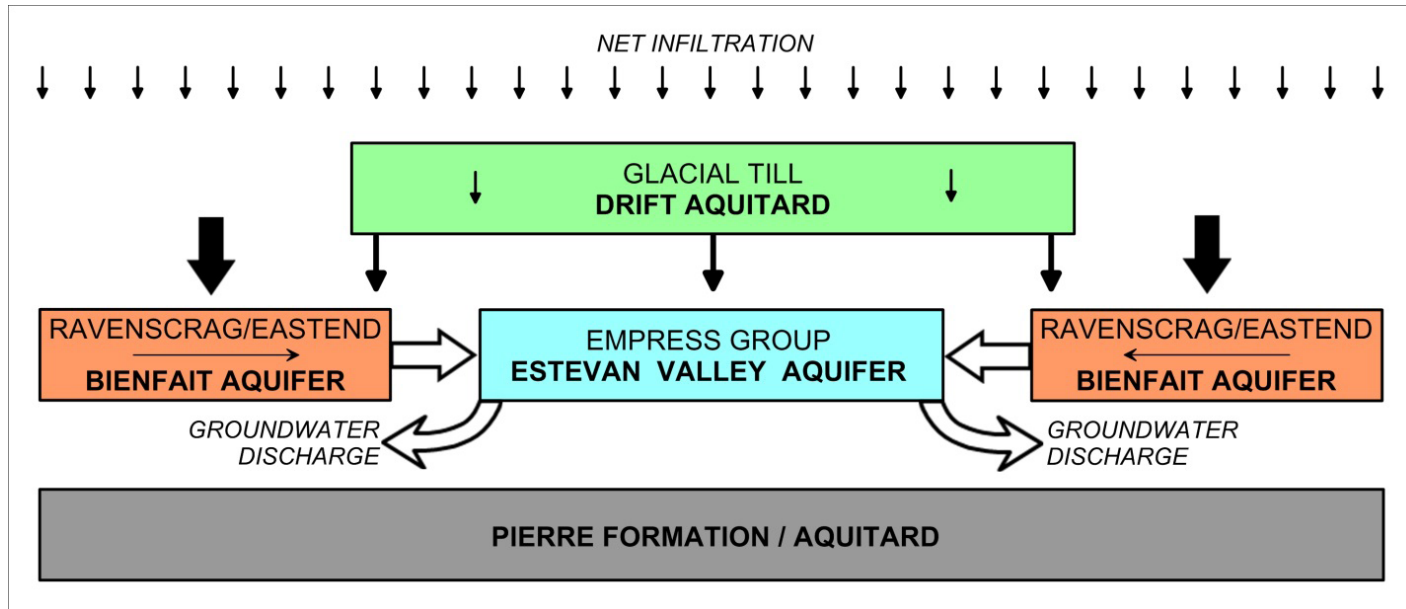


Figure 10: Schematic Diagram of Regional Groundwater Flow (Meneley, 1983)

Vertical leakage across the overlying Drift also contributes recharge into the EVA (Figure 10). The significance of this recharge relative to contribution from Eastend-Ravenscrag Aquifer may have been overstated in the past works and resulted in overestimated yields of the EVA. The low long-term yields and slow recovery of the EVA point towards a hypothesis that vertical recharge of the EVA across the overlying drift is a relatively minor component of the overall recharge into the aquifer.

The discharge areas of the EVA are likely further east; however, the exact mechanism and location of discharge are unknown. Meneley and Whitaker (1970) suggested that the discharge from the EVA is concentrated along the Souris River near Outram (Townships 3-4, Ranges 10-12) and Oxbow (Township 2-3, Ranges 1-3). However, there is no evidence to support these suggestions. Moreover, the artesian head in the EVA beneath Souris River valley (Meneley and Whitaker, 1970) points towards the presence of a competent aquitard overlying the EVA. Artesian

head and the hydraulic separation of the EVA from the surface are maintained under natural or undisturbed conditions.

The Eastend-Ravenscrag Aquifer is likely recharged by vertical flow through the overlying thinner tills and from upland areas or along limited outcrops in the southern parts of the study area. Groundwater flow in the shallower parts of Eastend-Ravenscrag Aquifer is likely controlled by local topography while deeper layers may be influenced by more regional flow.

Groundwater flow in the Eastend-Ravenscrag Aquifer is generally directed towards the EVA (both from north and south). The aquifer is hydraulically connected to the EVA as evident from the drawdowns induced by the withdrawals from the EVA. Locally, the Eastend-Ravenscrag Aquifer may also discharge in the low-lying areas including some parts of the Souris River. Hydraulic conductivity of Eastend-Ravenscrag Aquifer is highly variable due to lithological variations in the Ravenscrag-Eastend sequence and estimated to be 10^{-8} – 10^{-6} m/s (van der Kamp, 1985) and at least two orders of magnitude lower than EVA. Although the Eastend-Ravenscrag Aquifer appears to have relatively low hydraulic conductivity, flow out of the aquifer into the channel aquifer may be an important source of recharge to the EVA (Maathuis and van der Kamp, 1989).

3.4 Groundwater Quality

Groundwater chemistry in the Estevan, Yellowstone, and Missouri Channels is generally dominated by Na-HCO_3 type water, with low SO_4 , and 100 – 400 mg/L of Cl (Table 2, Figure 11). The sum of ions ranges between 1,000 – 2,000 mg/L. Higher and more variable mineralization is observed in the Northwest channel where groundwater is of Na-Cl/SO_4 type and sum of ions can be over 3,000 mg/L (e.g. wells M18UL-84 and M33U-90). Many of the EVA analyses indicate concentrations in excess of Saskatchewan's water quality objectives for sum of ions (or TDS), Na, Cl, Fe, and Mn. In many wells, including SaskPower's withdrawal wells, the maximum acceptable concentration of arsenic was exceeded by 2 – 4 times.

The Eastend-Ravenscrag Aquifer generally has higher mineralization than the EVA with the sum of ions typically greater than 2,000 mg/L. This aquifer is characterized by $\text{Na-HCO}_3/\text{Cl/SO}_4$ type water with notably lower hardness (Ca and Mg) than the EVA and intertill aquifers within the Drift. Groundwater within drift has even greater range of concentrations and water types than Eastend-Ravenscrag Aquifer. The overall hydrochemistries of these two groups have wide overlapping ranges making it difficult to determine which group contributes more to the recharge of the EVA.

Table 2: Concentrations of Major Ions in the Monitoring Well Network of EVA

Well	Aquifer	Sample Date	Ca	Mg	Na	HCO ₃ + CO ₃	SO ₄	Cl	Total Hard-ness	Sum of Ions
			mg/L	mg/L	mg/L	mg/L	mg/L	mg/L	mg/L	mg/L
PW1UL-88	EVA	9-Aug-88	48	23	405	867	<0.1	266	214	1,609
PW2U-88	EVA	31-Aug-88	37	21	388	834	<0.1	238	179	1,518
PW3UL-88	EVA	14-Dec-88	39	23	386	888	<0.1	216	192	1,552
PW4UL-84	EVA	17-Sep-84	52	23	386	965	<0.1	177	224	1,609
M10U-82	EVA	15-Nov-82	10	18	391	853	14	181	99	1,474
M11L-84	EVA	26-Jun-84	9	5	565	816	7	406	43	1,812
M12UL-84	EVA	25-Jun-84	10	16	423	742	7	230	91	1,434
M13UL-84	EVA	27-Jun-84	9	18	369	726	18	177	96	1,323
M14IT-84	EVA	25-Jun-84	23	42	244	592	14	194	230	1,117
M17U-84	EVA	23-Nov-84	32	10	430	1,030	2	162	121	1,672
M18UL-84	EVA	26-Jun-84	79	38	1,050	532	10	1,660	353	3,375
M19UL-84	EVA	29-Jun-84	46	22	390	801	14	300	205	1,580
M20U-84	EVA	3-Jul-84	13	12	408	783	10	247	82	1,479
M25UL-88	EVA	14-Jul-88	22	13	470	822	2	266	108	1,595
M28UL-88	EVA	23-Jul-88	43	18	510	1,120	22	140	181	1,861
M30UL-88	EVA	18-Aug-88	66	23	364	757	4	281	259	1,557
M32U-90	EVA	14-May-90	16	21	430	929	<10	231	126	1,627
M33U-90	EVA	11-Jun-90	26	9	817	964	468	488	102	2,773
M37U-93	EVA	8-Nov-93	69	39	510	1,073	3	419	332	2,123
M6L-82	EVA	15-Nov-82	6	5	564	772	67	322	36	1,764
M7U-82	EVA	15-Nov-82	107	31	344	432	735	57	395	1,725
M9L-82	EVA	15-Nov-82	34	17	494	947	8	350	155	1,855
R1UL-88	EVA	18-Jul-88	42	13	488	1,006	3	294	158	1,854
R3UL-88	EVA	26-Jul-88	41	22	533	1,180	19	129	193	1,924
R6UL-88	EVA	27-Aug-88	46	18	536	917	3	423	189	1,943
R7U-90	EVA	10-Jun-90	55	23	623	858	40	648	232	2,247
WSA Estevan	EVA	7-Aug-84	34	18	424	831	3	305	159	1,622
WSA Outram	EVA	8-Aug-84	36	14	412	1,020	2	174	147	1,664
M27ST-88	Tableland	19-Aug-88	160	112	528	695	1,370	56	859	2,921
R4ST-88	Hitchcock	2-Aug-88	48	32	534	699	736	44	251	2,093
M16R-84	East.-Rav.	25-Jul-84	5	4	1,300	572	8	1,730	29	3,620
M31R-88	East.-Rav.	31-Aug-88	20	6	1,000	587	16	1,260	75	2,904
M39R-93	East.-Rav.	13-Nov-93	5	2	650	845	625	45	21	2,174
M40R-93	East.-Rav.	14-Nov-93	20	10	840	901	74	794	91	2,649
M41R-93	East.-Rav.	16-Nov-93	11	3	920	910	3	975	40	2,826
R5R-88	East.-Rav.	19-Aug-88	8	9	566	895	271	140	57	1,889
M15IT-84	Drift	25-Jun-84	36	37	150	371	138	106	242	849
M24IT-88	Drift	19-Aug-88	132	66	245	628	349	172	601	1,604
M29IT-88	Drift	19-Aug-88	265	89	344	351	1,400	42	1,027	2,500
M5IT-82	Drift	16-Nov-82	8	57	178	281	402	37	254	978
M8IT-82	Drift	15-Nov-82	75	40	476	363	883	141	352	1,988
M38ST-93	Drift	10-Nov-93	71	38	295	1,016	20	95	333	1,542
R2IT-88	Drift	27-Aug-88	165	123	416	125	1,660	44	917	2,533

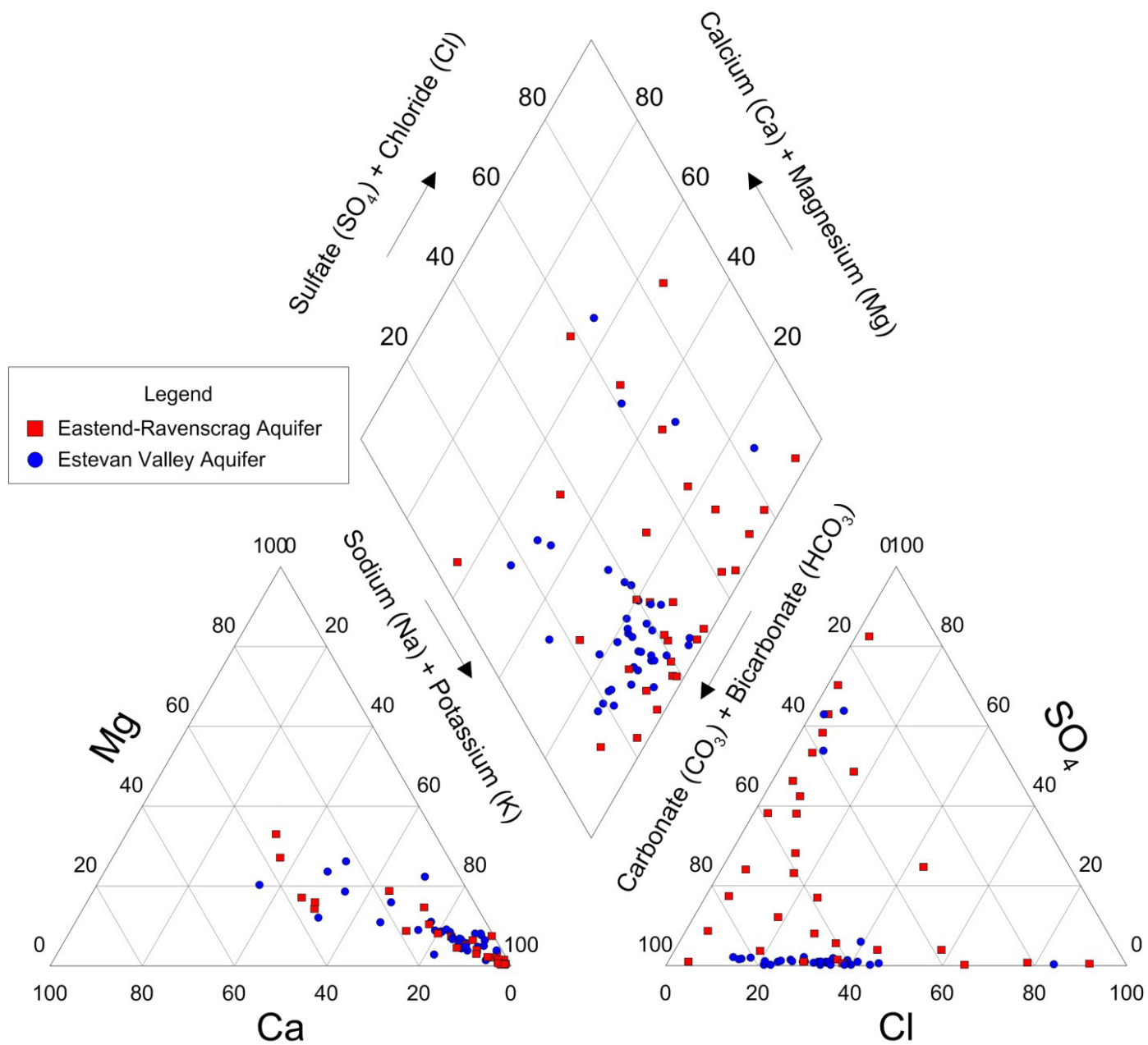


Figure 11: Piper Plot of Selected Chemistry Analyses

4.0 Groundwater Model

USGS Modflow code utilizing finite difference method (FDM) was selected for the development of this model. In the FDM method, the modelled domain is approximated by a grid consisting of rectangular cells. Each cell is assigned a hydraulic property and the hydraulic heads and fluxes at the center of each cell. Every cell is assigned to a model 'zone' (e.g. aquifer) and each zone has associated values of the horizontal hydraulic conductivity (K_h), vertical hydraulic conductivity (K_v), specific storage (S_s) and/or specific yield (S_y). Specific yield is assigned to the cell at the water table. Computer code then solves a set of algebraic equation generated by approximating the following governing equation:

$$\frac{\partial}{\partial x} \left(K_x \frac{\partial h}{\partial x} \right) + \frac{\partial}{\partial y} \left(K_y \frac{\partial h}{\partial y} \right) + \frac{\partial}{\partial z} \left(K_z \frac{\partial h}{\partial z} \right) - W = S_s \frac{\partial h}{\partial t}$$

where:

$K_{x,y,z}$ – hydraulic conductivity of the aquifer/aquitard along the x, y, and z directions (L/T),

h – hydraulic head (L),

W – sources or sinks of water (T^{-1}),

S_s – specific storage of the aquifer/aquitard (L^{-1}), and

t – time (T)

Visual MODFLOW software was used for its graphical interface during design, input, simulation, and calibration stages of the model.

4.1 Grid Discretization and Model Domain

The groundwater model domain includes TWP 1-5, RGE 4-13, West of the 2nd meridian, covering approximately 5,000 km². The FDM grid contained 120,000 cells (200 rows and 100 columns) within six layers. Horizontal dimensions of the cells were 500 × 500 m and remained uniform across the entire domain. The vertical dimensions of the cells varied from 0.1 m to 320 m due varying thickness of each formation. The approximate aquifer boundaries followed previous interpretations of the areal extent and from the additional borehole logs completed since 1994 (Van Stempvoort and Simpson, 1994).

During the validation stage and sustainable yield analysis, the grid was refined in the area of the SaskPower's production wells located at 03-10W2. The horizontal grid was refined resulting in cell dimensions of 50 × 50 m around the pumping wells. Vertical dimensions remained unchanged. This was done in order to better resolve aquifer response around the pumping wells and simulate more reasonable drawdowns in closely-spaced monitoring wells.

The development of the model layers was based on an updated geological framework. A type log, based on SaskPower's production well #4 (PW4UL-84), was created to illustrate the relationship between geology and hydrostratigraphy that were applied toward the development of groundwater model (Figure 12).

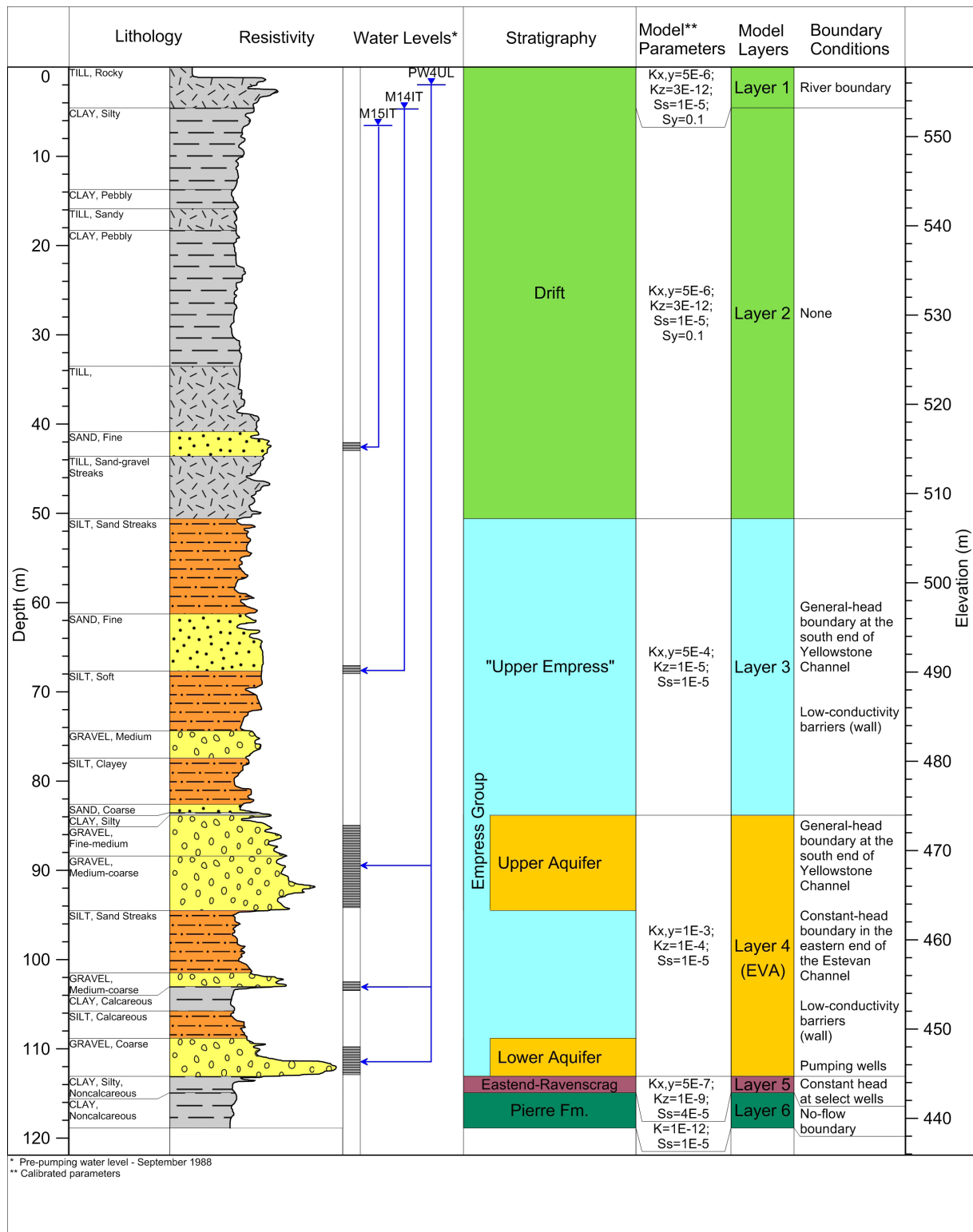


Figure 12: Type Log of Well PW4UL-84 Illustrating the Basis for Numerical Model

The model framework consisted of six (6) layers represented by:

- Drift Aquitard– Layers 1 and 2
- Upper Empress Aquifer – Layer 3
- Estevan Valley Aquifer – Layer 4
- Eastend-Ravenscrag Aquifer – Layer 5
- Pierre Aquiclude – Layer 6

The upper and lower gravel intervals *within the EVA* were initially referred to as “Upper Aquifer” and “Lower Aquifer”, respectively, by Beckie and Pasloske (1985) (Figure 12). However, they were combined into one model layer (EVA) due to hydraulic continuity and combined production from both intervals.

The Tableland and Hitchcock aquifers were excluded from this model. Although there are very limited monitoring data to completely rule out any connectivity to the EVA, the geologic maps and cross-sections as well as water quality suggest that Tableland and Hitchcock aquifers are not directly hydraulically connected to the Estevan Valley Aquifer. The elevation of the lowest point (the bottom) of the Tableland/Hitchcock aquifer is at least 20 m higher than the top of the Empress Group in the Estevan Channel and separated by till. Furthermore, Tableland aquifer response to pumping was distinctly different from the response of the EVA as discussed in Maathuis and van der Kamp (1998).

Although the conceptual model combined the Sutherland and Saskatoon Group aquifers into a single hydrostratigraphic unit (Drift Aquitard), it was separated into two modelled layers (Layers 1 and 2) in order to accommodate surficial boundary conditions and maintain vertical gradient across the aquitard. The thickness of Layer 1 is arbitrary and represents 10% of total thickness of Drift Aquitard at any given location. Layer 2 represents the remaining 90% of aquitard’s thickness. Hydraulic properties of both layers remained identical in order to maintain consistency with the conceptual model.

In the EVA model development, the major groundwater system is represented by Layer 3 and Layer 4 due to the hydraulic connection between these layers. Layer 5 is represented by the Eastend-Ravenscrag aquifer belonging to the Eastend to Ravenscrag Formations.

The Pierre Formation (Layer 6) was considered an aquiclude in the model development. All cells within Layer 6 were assigned a no-flow boundary to eliminate any contribution of groundwater from beneath the EVA or Eastend-Ravenscrag Aquifer. The thickness of Layer 6 was set to 1 m across the entire model domain.

4.2 Boundary Conditions

Steady-state simulation requires specification of boundary conditions (Figure 13). These boundaries largely determine the steady-state flow-pattern and have influence on the transient solution if/when the effects of stress reach these boundaries.

4.2.1 Simulation of Rivers

One major river (Souris River) and a small tributary (Long Creek) extending from northwest to southeast of the model domain were incorporated in to the numerical groundwater model (Figure 13). The Souris River was simulated by specific head equal to the surface elevation of each corresponding cell. The specific head cells allow the surface water to be hydraulically connected to the groundwater without any restrictions or leakage factor. It is expected that the river boundary condition would provide the necessary recharge into the system. For this reason, no additional areal recharge was applied across the domain.

The hydrologic information of the Souris River within the model domain was estimated due to a lack of detailed information of the river in this area. The bottom of the river was assumed to be 2 m below the river stage corresponding to each cell. Riverbed thickness was established at 1 m and the average width of the river at 200 m. The vertical hydraulic conductivity parameter was set to 10^{-6} m/s (silt or silty sand, Freeze and Cherry, 1979) with the assumption that the bottom river sediments comprised of alluvium, silts, and clays.

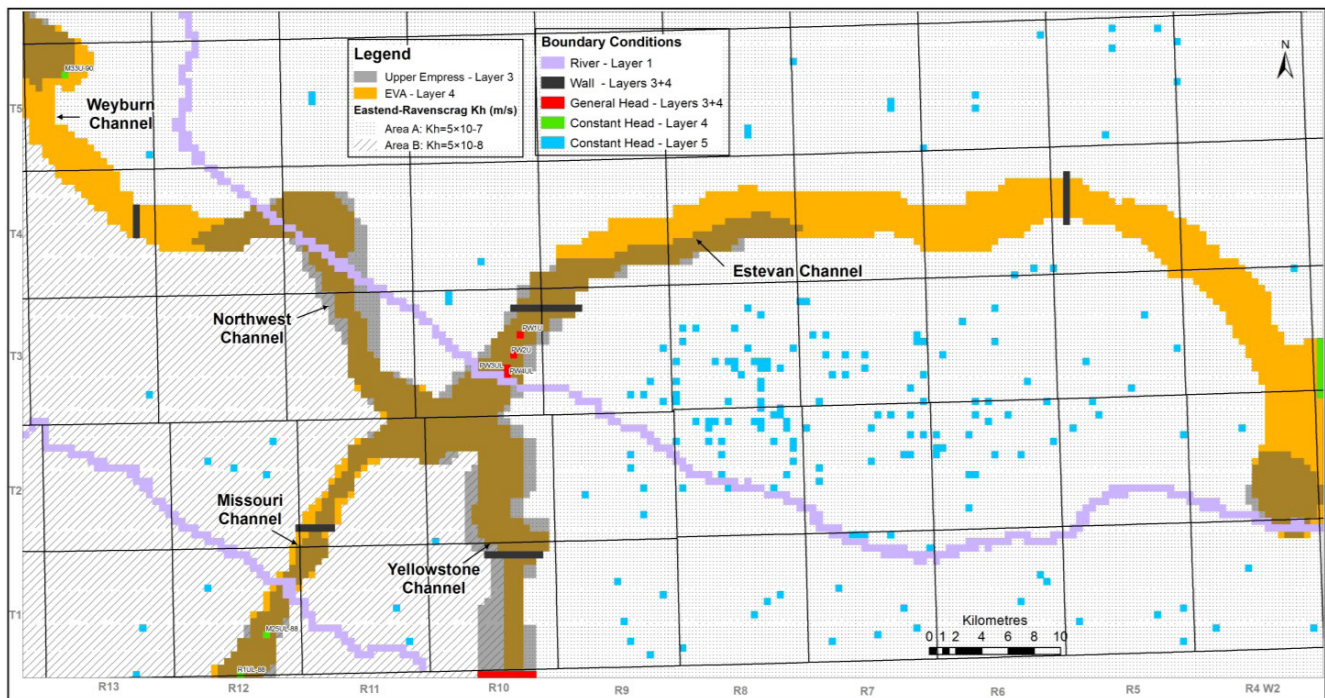


Figure 13: Model Boundary Conditions

4.2.2 Constant Head

Constant-head boundary condition of 535 m was applied to Layers 3 and 4 (Upper Empress and EVA) at the eastern end of the Estevan Channel (Figure 13). This boundary condition was needed to control hydraulic head at the eastern edge of the channel and facilitate groundwater outflow from the model domain.

Constant-head boundary conditions were also applied at wells R1UL and M25UL in the Missouri Channel (605.82 m and 605.23 m, respectively) and well M33U in the Weyburn Channel (564.00 m). These boundaries are reasonable because these wells showed limited response to drawdowns from pumping of the EVA due to the inferred hydraulic discontinuities. The hydraulic discontinuities will also limit the infinite supply of water created by this boundary condition from flowing into the EVA.

Constant-head boundary conditions were applied at selected domestic wells in Layer 5 (Eastend-Ravenscrag Aquifer). The hydraulic heads used for these constant-head boundary conditions represent static values from domestic wells reported to WSA by water well drillers. While it is recognized that some of the hydraulic head values may not be representative of static conditions, overall they appear to be generate reasonable approximation of regional hydraulic gradients.

No drawdowns were observed in the Eastend-Ravenscrag Aquifer beyond 4,500 m from the edge of EVA (Table 3). Constant head boundary conditions were applied only at the domestic wells that are located outside of the 5,000 m buffer zone around the EVA in order to prevent the transient drawdowns from reaching the boundary conditions. The increased setback distance was also chosen to account for uncertainty the position of the channel. Subsequent transient modelling would show that a drawdown of 1 m did not extend more than 4,500 m from channel's edge in areas closest to the production wells; thus, did not reach the constant-head boundary conditions. It is important to note that modeling of pumping scenarios using higher withdrawal rates ($> 4,143$ dam³/year) or longer duration (> 5 years) may result in drawdowns reaching the boundary conditions in the Eastend-Ravenscrag Formation. In this case, the model's boundary conditions will need to be reconsidered given the specifics of a particular scenario.

Table 3: Maximum drawdown in Eastend-Ravenscrag Monitoring Wells after Five (5) Years of Pumping (Maathuis and van der Kamp, 1998)

Observation Well	Distance from Channel's Edge (m)	Maximum Drawdown (m)
M16R-84	<500	22
M35R-92	700	13
M36R-92	2,500	2
M41R-93	3,400	1
R5R-88	4,500	0

4.2.3 General Head

The use of constant head may potentially introduce an unlimited supply of water into the aquifer. A flux boundary or general-head boundary condition can be used to modify flux entering and leaving the selected cells. This is a head-dependent flux boundary also known as mixed or Cauchy boundary condition. This boundary condition was applied to Layers 3 and 4 at the south end of Yellowstone Channel at the International border (Figure 13). The value of specified head was set to 570 m at a distance of 10 km south of the international border. These values are based on observations at wells 163-097-24AAA and 163-097-25AAA located near Crosby, North Dakota.

Four pumping wells, representing flux boundaries, were completed in Layer 4.

4.2.4 Inferred Hydraulic Discontinuities

Barrier walls were applied to Layers 3 and 4 (Figure 13). Four low conductivity barrier walls were positioned in the Missouri, Northwest Channels, and Estevan Channels. The location of these hydraulic discontinuities was estimated based on previous investigations (Maathuis and van der Kamp, 1998). These walls simulate hydraulic discontinuities in the aquifer.

To improve calibration at the international border, additional barrier wall was added in the Yellowstone Channel. The position of this barrier is approximate and similar effect (calibration) could be achieved by varying hydraulic properties of the aquifer in the Yellowstone Channel. However, in the absence of aquifer/pumping tests in this area, the wall boundary condition was the preferred type of boundary condition.

The properties of these walls were determined by trial-and-error at the calibration stage and are summarized in Table 4.

Table 4: Parameters of Barrier Walls

Wall Location	Township-Range	Thickness (m)	Hydraulic Conductivity (m/s)
Missouri Channel	02-11W2	500	1E-8
Northwest Channel	04-13W2	500	1E-8
Yellowstone Channel	01-10W2	500	8E-6
Estevan Channel (west)	03-09W2, 03-10W2	500	7E-6
Estevan Channel (east)	04-05W2	500	1E-5

4.2.5 Initial Conditions and Parameters

For the steady-state model, initial heads were assigned to all layers based on pre-production hydraulic head data. The values of hydraulic head at the water table were approximated by the topographic surface from the DEM and applied to Layers 1 and 2. Pre-pumping hydraulic heads from the EVA were manually contoured and applied to Layers 3 and 4. Hydraulic heads from Eastend-Ravenscrag Aquifer were manually contoured and applied to Layer 5.

The following initial hydraulic properties were assigned to each layer:

Table 5: Initial Parameters

Property	Layer 1	Layer 2	Layer 3	Layer 4	Layer 5	Layer 6
K_x (m/s)	5×10^{-9}	5×10^{-9}	1×10^{-5}	1×10^{-5}	5×10^{-7}	1×10^{-12}
K_y (m/s)	5×10^{-9}	5×10^{-9}	1×10^{-5}	1×10^{-5}	5×10^{-7}	1×10^{-12}
K_z (m/s)	1×10^{-11}	1×10^{-11}	1×10^{-6}	1×10^{-6}	1×10^{-12}	1×10^{-12}
S_s (m-1)	1×10^{-6}	1×10^{-6}	1×10^{-6}	1×10^{-6}	1×10^{-6}	1×10^{-6}
S_v	0.1	0.1	0.2	0.2	0.1	0.1
Eff. Porosity (%)	10	10	20	20	20	10

These properties are based on and within the ranges of values used by Maathuis and van der Kamp (1989) and Lu and Jin (2002).

For transient model, initial heads were assigned to all layers based on the output of hydraulic heads from the steady-state model. Any change in input parameters resulted in different steady-state heads and, thus, different initial heads for transient simulations. Every transient simulation was preceded by a corresponding steady-state simulation.

The use of model-generated heads as initial head values ensures that the initial head data and the input parameters are consistent during transient simulation (i.e. in hydraulic equilibrium). Meaning, the simulated transient changes in hydraulic heads are only due to the applied aquifer stress and not affected by model's adjustment to boundary conditions and input parameters. However, it should also be recognized that some adjustment to boundary conditions and input parameters will occur during the calibration stage of the transient model. This uncertainty cannot be eliminated due to the interdependency of steady-state and transient simulations.

4.3 Simulation Runs

Simulations were first run in steady-state condition with pumping wells deactivated. This established pre-pumping steady-state heads. The start date for transient simulations was set on September 16, 1988, with a simulation period of 9,968 days (until January 1, 2016). Heads from the preceding steady-state simulations were set as initial heads for the transient simulations.

MODFLOW automatically established the number of pumping periods based on the pumping schedule for each well, which is based on monthly rates and volumes reported by SaskPower. A total of 65 pumping periods from day 0 (September 16, 1988) to day 2076 (May 24, 1994) were established with each period having multiple time steps. A single recovery period was established from day 2076 (May 24, 1994) until day 9968 (January 1, 2016). A multiplier of 1.2 was used during the recovery period to establish 15 time steps weighted towards early recovery time.

Model was run using WHS solver with following settings:

- Maximum outer iterations – 1000
- Maximum inner iterations – 500
- Head change criterion – 0.1
- Residual criterion – 0.1
- Damping factor – 0.8-1
- Relative residual criterion – 0

Numbers of outer and inner iterations were increased over the default values in order to avoid potential non-convergence due to insufficient iterations. Head change and residual criteria were also increased within reasonable range to speed up the convergence. Damping factor was reduced to 0.8 (default is 1) to avoid non-convergence due to oscillations and divergence that occurred during some simulation runs.

4.4 Calibration

Calibration of any regional model is a difficult task given the relatively sparse data/knowledge compared to the size of the model domain and the range of observed heads. Therefore, a certain degree of subjective judgement combined with statistical analysis should be used to measure the quality of calibration. Calibration of this model was performed using both manual (trial-and-error) and automated techniques. Two measures of steady-state calibration were considered:

1. Root Mean Squared (RMS) is defined as the average of the squared differences between measured (h_m) and simulated heads (h_s): The RMS is regarded as the best estimate of ‘closeness’ to the observed variable, assuming that the errors are normally distributed (Anderson and Woessner, 1992).

$$RMS = \sqrt{\frac{1}{n} \sum_{i=1}^n (h_m - h_s)^2}$$

The RMS is normalized by dividing RMS by the difference between the maximum and minimum observed head values:

$$NRMS = \frac{RMS}{(h_m)_{max} - (h_m)_{min}} \times 100\%$$

Normalized Root Mean Squared (NRMS) value of less than 10% would constitute a calibrated model. NRMS is a standard criterion typically employed in industry. However, it should be noted that NRMS is a good measure of error (residual) if the errors are distributed normally. This may not be the case because of a monitoring bias towards the pumping wells (i.e. 65% of EVA monitoring wells are within 10 km radius of pumping wells). Also, NRMS can vary depending on the range of hydraulic heads in the data points that are included in calibration. For these reasons, a second, qualitative measure of calibration was also necessary.

2. Residual value is the difference between observed and modelled/calculated hydraulic head. A residual cut-off value of ± 1 m was chosen as the subjective measure of acceptable calibration of the steady-state model. Given the low gradients observed in the EVA, as well as possible errors in the measurement of hydraulic heads, well locations, and reference elevations, the residuals of less than 1 m would be considered acceptable for successful steady-state calibration.

Quantitative measures, such as NRMS, were also used to evaluate the calibration of transient model. NRMS values were calculated for every time step during the stress period. In addition, an analysis of calculated versus observed drawdowns and heads (hydrographs) were undertaken because NRMS alone does not provide sufficient evidence of whether the model was able to reproduce the general trends observed during the stress period. Ultimately, the judgement of the calibration quality is highly subjective based on professional interpretation of the data.

4.4.1 Steady-State Results

Initial (pre-production) steady-state model was calibrated using automated parameter estimation analysis (PEST) by varying hydraulic conductivities of Layers 3 and 4 until the best fit was obtained between steady-state model heads and pre-pumping heads at 12 selected monitoring locations (Table 6). These wells were selected along the channel in order to minimize kurtosis of the data. Monitoring locations were chosen such that they are more or less evenly distributed throughout the length of channel. Adjusted parameters were applied to Layers 3 and 4 and the steady-state model was re-run to produce the final output. This calibration procedure resulted in correlation coefficient of 0.997 and NRMS of 1.538%.

Subsequent transient simulations have shown that the parameters obtained during steady-state calibration were not able to reproduce drawdowns from pumping. Therefore, parameters were manually re-adjusted through trial-and-error until both transient and steady-state model were able to reasonably reproduce the observed data. This resulted in poorer but still acceptable calibration of the steady-state model: correlation coefficient of 0.995 and NRMS of 2.8% (Table 6 and Figure 14).

Calibrated hydraulic heads and residuals were contoured and shown on Figures 15 and 16, respectively. Overall, the steady-state model appears to be representative of the pre-pumping distribution of hydraulic heads in the EVA. Groundwater flow is generally directed into the Estevan Channel, towards east and northeast. The differences between modelled and observed hydraulic heads are within the ± 1 m criterion throughout most of the aquifer (Figure 16). Calibrated results show that approximately 99% of the simulated area is within the criterion. Uncertainties of more than 2 m exist at the international boundary.

Unsuccessful attempts have been made to reduce the errors in the Yellowstone Channel by varying hydraulic conductivities of the EVA and the inferred discontinuities (barrier wall) and properties of the general-head boundary condition. Any additional adjustments to hydraulic properties that reduced errors in this area have also resulted in the overall poorer calibration throughout the rest of the modelled domain. Thus, no further attempts to improve steady-state calibration in this area have been made.

Table 6: Steady-State Calibration Data

Well ID	Observed Head (masl)	Calculated Head (masl)	Residual (m)
M04U-82	554.290	554.791	0.501
M06L-82	557.640	557.689	0.048
M07U-82	554.335	554.030	-0.305
M11L-84	557.389	557.511	0.122
M17U-84	557.266	557.341	0.075
M18UL-84	557.823	557.596	-0.228
M19UL-84	556.995	556.971	-0.024
M20U-84	557.566	557.637	0.071
M28UL-88	561.650	560.952	-0.698
M37U-93	537.840	537.767	-0.073
R3UL-88	563.290	561.188	-2.102
R6UL-88	553.460	552.644	-0.816

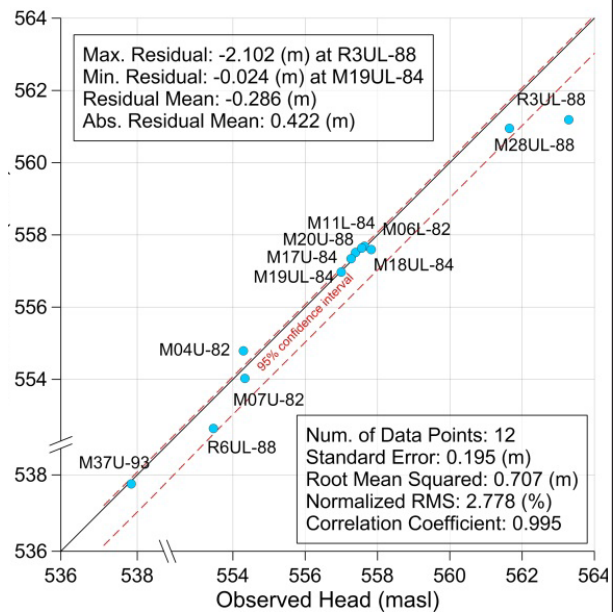


Figure 14: Steady-State Calibration Plot

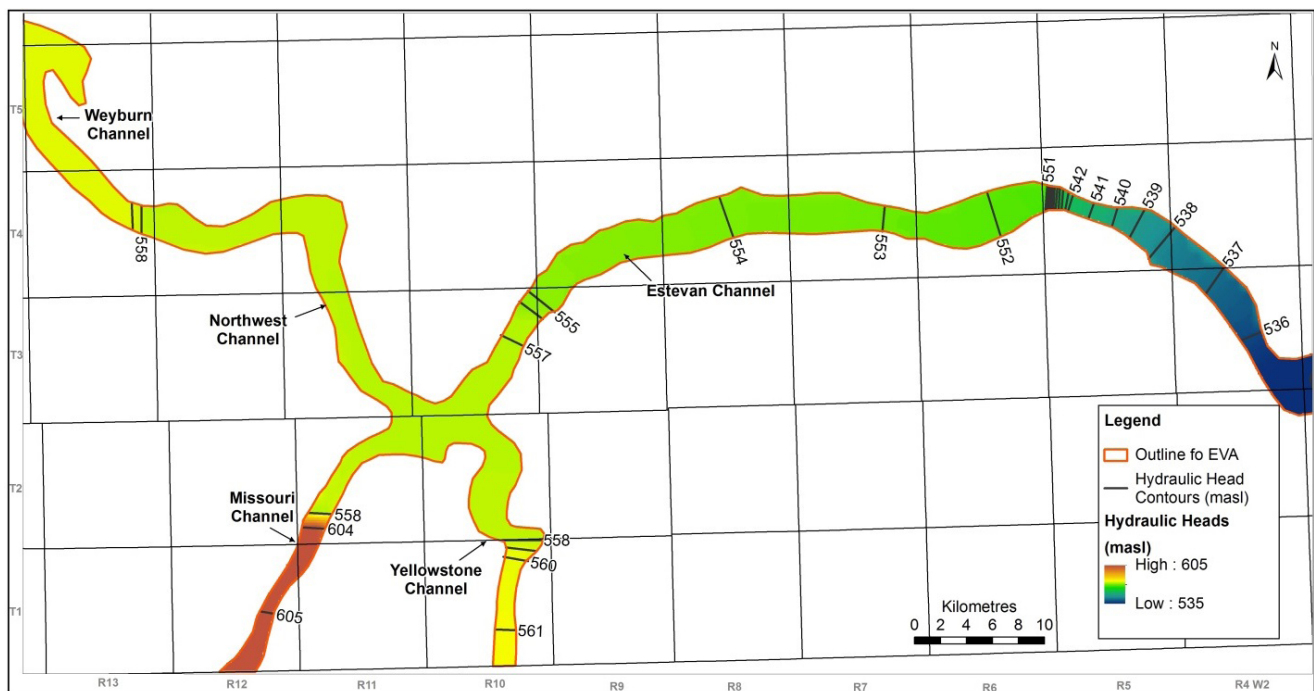


Figure 15: Steady-State Hydraulic Heads in the EVA (Layer 4)

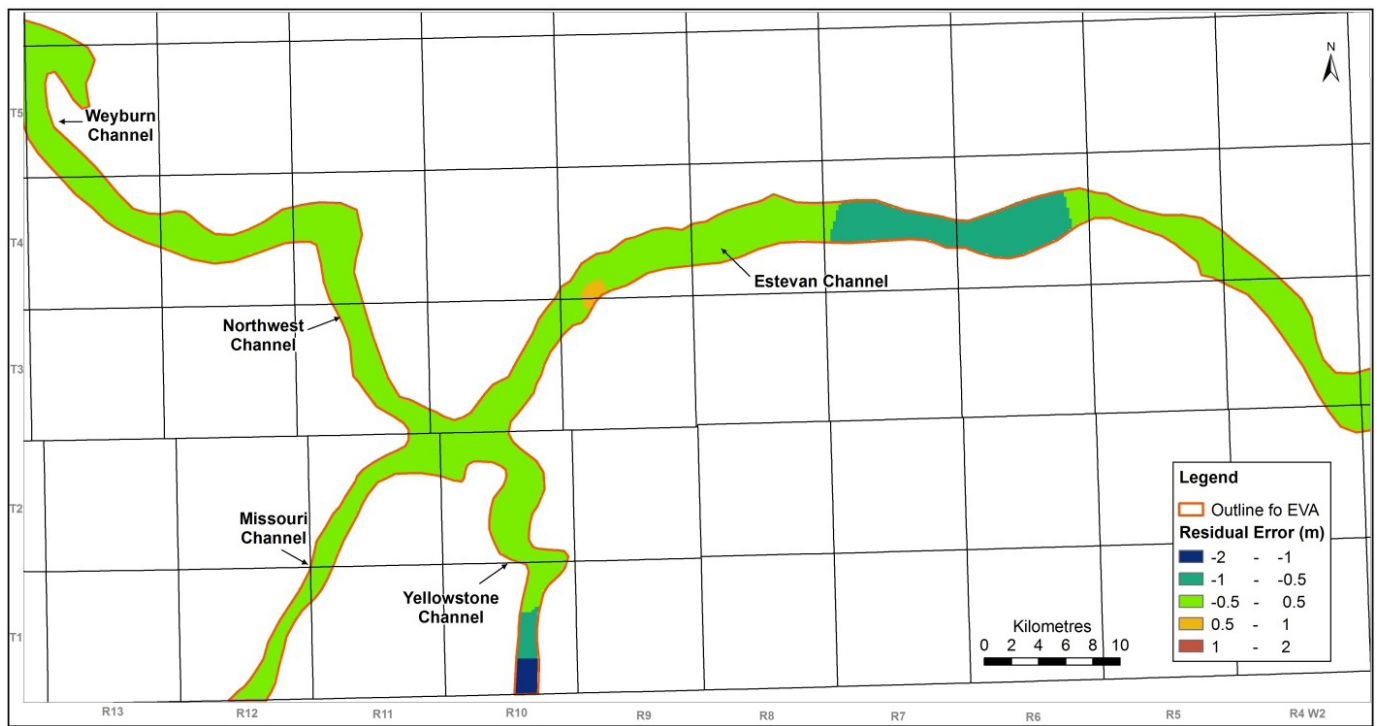


Figure 16: Distribution of Steady-State Residual Errors in the EVA (Layer 4)

4.4.2 Transient Results

Transient model was manually calibrated to the pumping period (September 16, 1988 – May 24, 1994) using water level data from wells completed in Empress Group (Layers 3 and 4). Drawdown data from 24 wells completed in the Empress Group were used for transient calibration (Table 7).

Four existing monitoring wells were not used for transient calibration for the following reasons:

- R1UL-88 and M25UL-88 – located in Missouri Channel, showed limited response to pumping, and were used for constant-head boundary conditions.
- M33U-90 – located in Weyburn Channel and showed limited response to pumping.
- M32U-90 – showed anomalously low response to pumping for unknown reason.

Hydrographs for wells WSA ESTEVAN and WSA OUTRAM are shown on Figure 17 and hydrographs of all other monitoring wells can be found in Appendix B. Each well has two associated graphs: drawdown and water level (hydrograph). It should be noted that the observed (actual) drawdowns could not be calculated for wells that were installed after September 16, 1988, due to the lack of initial (pre-pumping) water level.

Transient calibration statistics show that 20 out of 22 wells (with sufficient data) have NRMS of < 10%. Wells R3UL-88 and R7UL-90 had poorest calibration results of 14.8% and 10.7% NRMS error, respectively. Well R3UL-88 (Figure B.21) is located in the Yellowstone Channel at the international border and its poor transient calibration is likely the consequence of poor steady-state calibration since the heads from the steady-state model were used as input for the transient model. Well R7UL-90 (Figure B.23) is located in the Northwest Channel, furthest west

from the production site. Poorer calibration at this location may be due to unresolved geology and aquifer heterogeneity. Nevertheless, the model is still able to estimate the long-term drawdowns (general trends and magnitude) in all wells reasonably well.

Table 7: Statistics Measures of Transient Calibration

Well	# of Data Points	Standard Error of Estimate (m)	Root Mean Squared (m)	Normalized RMS (%)	Correlation Coefficient	Maximum Residual (m)	Residual Mean (m)	Absolute Residual Mean (m)
GSC3AL-60	78	0.032	0.532	2.980	0.999	-0.938	-0.450	0.493
M04U-82	97	0.059	0.780	3.339	0.998	1.860	0.529	0.605
M06L-82	94	0.140	1.482	4.147	0.994	3.528	0.608	1.244
M07U-82	90	0.043	0.696	3.879	0.997	-3.539	-0.566	0.587
M09L-82	92	0.220	2.184	4.869	0.988	-4.874	-0.597	1.774
M10U-82	92	0.278	2.785	5.850	0.982	7.169	0.847	2.291
M11L-84	105	0.138	1.462	3.916	0.993	4.746	0.391	1.180
M12UL-84	98	0.259	2.719	5.851	0.983	6.897	0.948	2.230
M13UL-84	91	0.299	3.168	6.685	0.980	9.116	1.407	2.614
M17U-84	104	0.215	2.320	5.265	0.988	5.859	0.798	1.884
M18UL-84	89	0.097	1.269	4.364	0.996	-2.728	-0.881	1.087
M19UL-84	96	0.313	3.059	6.378	0.977	7.938	0.277	2.527
M20U-84	70	0.119	1.001	3.063	0.996	2.185	-0.175	0.806
M21UL-86	80	0.322	2.889	6.118	0.981	-9.008	-0.391	2.392
M22UL-88	93	0.336	3.735	7.494	0.971	-10.499	1.270	3.101
M23UL-88	96	0.327	3.236	6.708	0.976	8.247	0.568	2.723
M28UL-88	87	0.192	1.788	8.097	0.983	4.330	0.123	1.487
M30UL-88	92	0.077	0.898	3.721	0.996	-2.240	0.519	0.684
M34U-92	16	0.088	0.765	Insufficient data		-1.564	-0.684	0.684
M37U-93	6	0.193	1.213	Insufficient data		-1.396	-1.133	1.133
R3UL-88	45	0.185	2.803	14.833	0.979	-5.299	-2.522	2.546
R6UL-88	56	0.085	0.937	6.780	0.993	-2.861	-0.693	0.771
R7UL-90	37	0.183	1.100	10.714	0.998	-1.749	0.015	1.004
TW1L-65	68	0.087	1.011	4.630	0.995	2.211	0.720	0.763

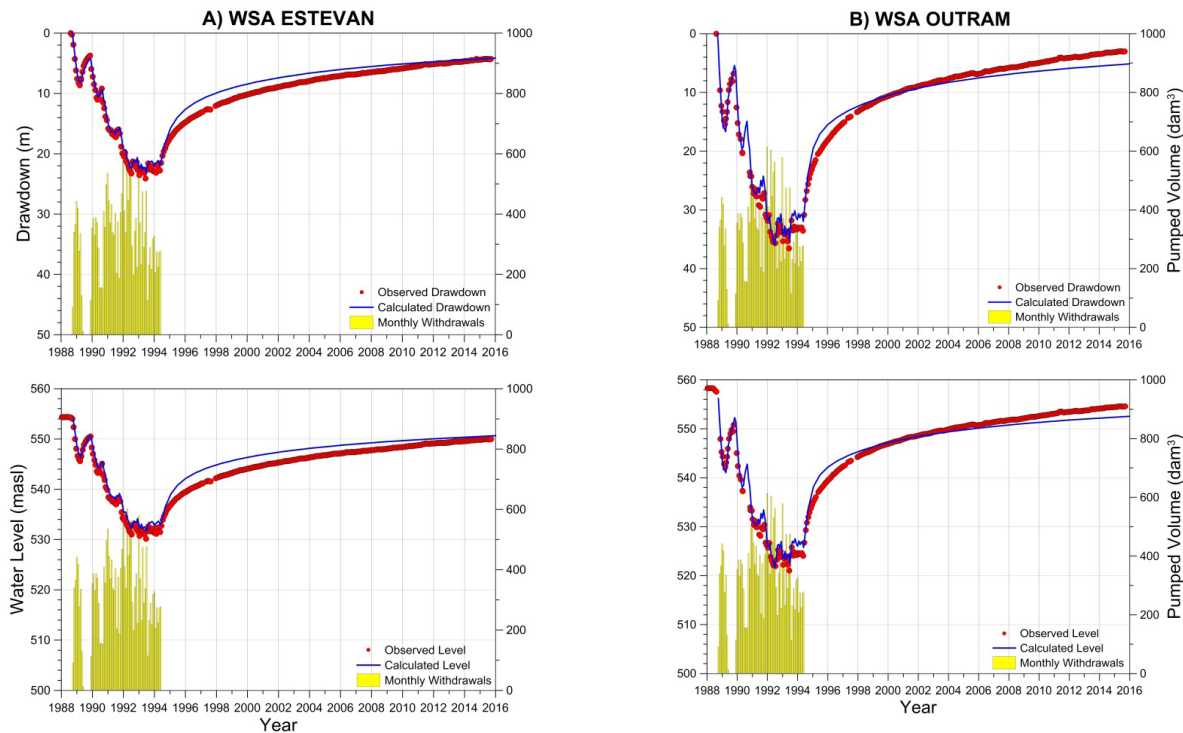


Figure 17: Hydrographs and Drawdowns of Wells WSA ESTEVAN and WSA OUTRAM

Hydrographs of wells with complete record of recovery data (WSA ESTEVAN and WSA OUTRAM, Figure 17) show that the model has *overestimated* early recovery and *underestimated* late recovery by up to 4 m. Both modelled and observed data show incomplete recovery even after 20 years since pumping ceased. This is consistent with previous results from Maathuis and van der Kamp (1998).

In addition to the individual wells, the NRMS values were calculated for each simulated time-step during pumping period (Figure 18). The transient model has greatest uncertainty during the recovery periods after the pumping stops or pumping rate is reduced. The NRMS error for this period ranged between 10% and 18%, values that are typically considered unacceptable. When the pumping rate was maintained relatively constant or its changes were gradual, the NRMS error was reduced to 4 – 10%. The average NRMS error for all time steps was calculated to be 7% and is considered to be acceptable.

The model was also run using average pumping rate and modelled drawdowns were compared to observed drawdowns in selected locations. The wells were pumped for a total of 1,880 days (or 5.15 years) at an average rate of 4,143 dam³/year. Note that the calculation of this rate excluded the short recovery period in 1989. The results of this simulation are presented in Table 8 and show that the discrepancy between the modelled and calculated drawdowns is less than 1 m, including at the international boundary (R3UL). This suggests that despite the poor steady-state calibration at this location, the model is capable of estimating overall transient drawdowns in the EVA.

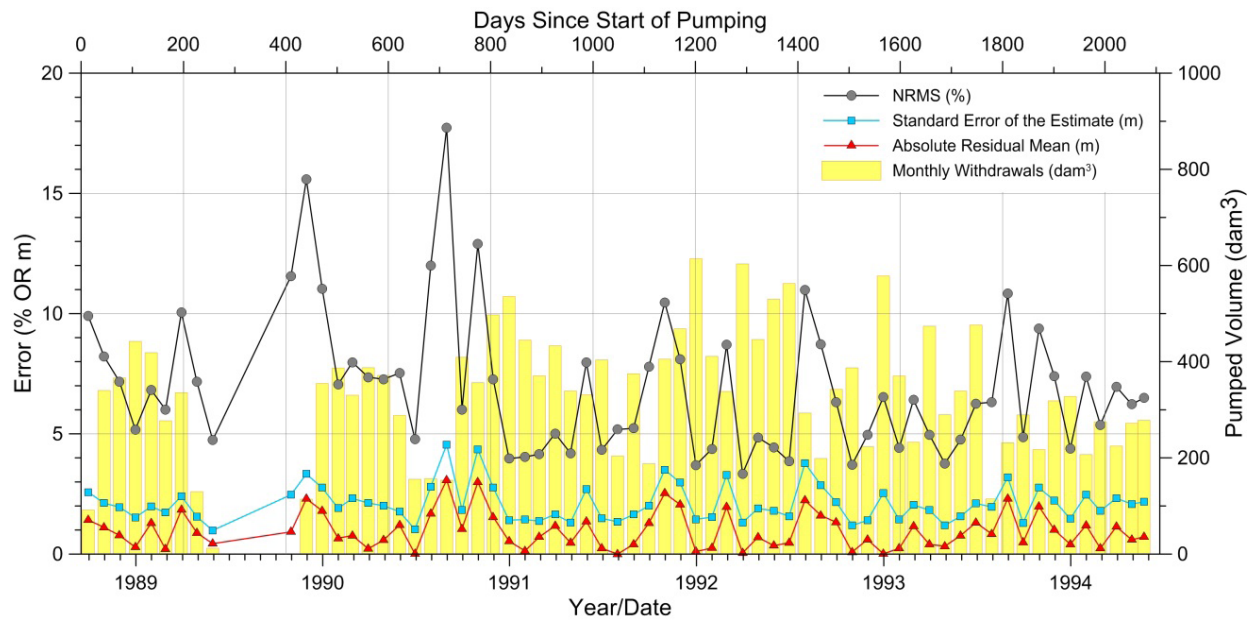


Figure 18: Average Errors per Time Step of Transient Simulation

Table 8: Comparison of Observed and Modelled Drawdowns Assuming Average Pumping Rate

Type	Days	Years	Average Pumping Rate (dam ³ /yr)	Drawdowns					
				Pumping Wells (m)*	WSA Estevan (m)	WSA Outram (m)	R3UL (m)	R7UL (m)	R6UL (m)
Observed	1,880	5.15	4,143	45	22	33	19.5	23	14
Modelled	1,880	5.15	4,143	44	22.5	34	19	24	13

*Average drawdown for all pumping wells at the end of pumping period.

4.4.3 Calibrated Parameters

Table 9 shows parameters that were adjusted to calibrate the model. Most parameters were adjusted within one order of magnitude of their initial values. The Eastend-Ravenscrag Aquifer (Layer 5) was split into two zones of different hydraulic conductivities. These zones are shown on Figure 13. Zone A represents the aquifer to the north and east of the channels. Zone B represents the southwestern portion of the model domain and has lower hydraulic conductivity than Zone A. The reduction in hydraulic conductivity of Zone B was necessary in order to counteract the increased hydraulic gradient in the southwest due to increase in topography. This limited the flux increase due to greater elevation and improved calibration of the EVA, particularly in the Northwest Channel.

Table 9: Calibrated Parameters (changes highlighted in red)

Property	Layers 1 & 2	Layer 3	Layer 4	Layer 5 (A)	Layer 5 (B)	Layer 6
K_x (m/s)	5×10^{-10}	5×10^{-4}	1×10^{-3}	5×10^{-7}	5×10^{-8}	1×10^{-12}
K_y (m/s)	5×10^{-10}	5×10^{-4}	1×10^{-3}	5×10^{-7}	5×10^{-8}	1×10^{-12}
K_z (m/s)	3×10^{-12}	1×10^{-5}	1×10^{-4}	1×10^{-9}	8×10^{-10}	1×10^{-12}
S_s (m ⁻¹)	1×10^{-5}	1×10^{-5}	1×10^{-5}	4×10^{-5}		1×10^{-5}
S_y	0.1	0.2	0.2	0.1		0.1
Eff. Porosity (%)	10	20	20	20		10

4.5 Mass Balance

The mass balance is one of the the key indicators of a successful simulation. The mass balance errors (difference between inflow and outflow) for steady-state and transient models was less than 0.5% with most values being less than 0.1%. The mass balance error of less than 2% generally suggests that the simulation is acceptable and without major instabilities in the solution or inconsistencies in the results. The mass balance also provides information about the water sources/sinks in the model. The relative magnitude of water volumes passing through these sources/sinks can point towards sources of greatest errors and improve understanding of the model's response to changes.

4.5.1 Steady-state

The steady-state simulation depends entirely on specified boundary conditions. Thus, in steady-state, all water enters and exits the domain via the boundary conditions independent of time. The model Mass balance output of the steady-state simulation shows that:

- 68% of water is sourced from constant-head boundary conditions within Ravenscrag-Eastend formations as supported by the water level measurements at well M16R-84.
- 31.5% of water is sourced from general-head boundary condition in the EVA at the international border.
- 0.5% of water is sourced from river boundary condition (leakage across aquitard).

These proportions show that the input from the river boundary condition (or recharge) has little overall impact on the steady-state simulation compared to the input from constant- or general-head boundary conditions. This result may be acceptable for this particular model; however, its actual regional applicability is unknown due to uncertainties in the model's input parameters.

4.5.2 Transient state

The results of the transient mass balance for the entire duration of withdrawals by SaskPower are documented in Table 10. The negative change in volume is indicative of water loss and the positive change indicates water gain. For example, 20,115 dam³ was lost from storage while 21,339 dam³ was gained by wells.

Table 10: Mass Balance of the Calibrated Model at the End of Pumping Period

Source	Volume IN (dam ³)	Volume OUT (dam ³)	Change in Volume (dam ³)	Per cent
Storage	31,199	11,084	-20,115	-92.6%
Constant-Head	21,302	21,675	373*	+100%
Wells	0	21,339	21,339	
River	846	823	-23	-0.1%
General-Head	1,594	0	-1,594	-7.3%
Total	54,941	54,922	-19	

*Some water was gained by the eastern constant-head boundary condition in the EVA, which suggests that drawdowns have not reached this boundary condition.

The transient mass balance shows that almost 93 % of extracted water was sourced from storage and less than 0.1 % was sourced from river leakage via the aquitard. This also suggests that impacts on the surface water from SaskPower's withdrawals are negligible. It is not possible to determine the contribution of each unit, but it is likely that most water was sourced from EVA's storage (at least during the early pumping times), and the remainder was sourced from the Eastend-Ravenscrag Aquifer and the overlying tills.

4.6 Sensitivity Analysis

The greatest uncertainty of the model is in the boundary condition and aquifer properties. However, it would be impossible to create numerical model without making any assumptions or simplifications. Sensitivity analysis is required in order to quantify the uncertainty in the calibrated model caused by estimated hydraulic parameters and boundary conditions and identify the parameters that influence the model results most.

Sensitivity analysis measures the change in model output associated with the change in model input (e.g. parameter values). During a sensitivity analysis, calibrated values of hydraulic parameters are varied, one parameter at a time, and the model's response is documented in terms of changing head or error (e.g. NRMS). Quantitative sensitivity analysis can then be performed by calculating sensitivity coefficients or sensitivities. However, given the large/regional scale of the model and the geological uncertainty, it was decided to perform only visual or qualitative analysis of model's sensitivity.

The detailed results of the model sensitivity runs can be found in Appendix C. For steady-state analysis, hydraulic conductivity values of all layers varied by 0.01 – 100 times of the calibrated parameters. Sensitivity to storage was not assessed since the steady-state simulation excludes any changes to storage, by definition. For transient-state analysis, hydraulic conductivity and specific storage values varied 0.1 – 10 times of the calibrated parameters. The shown NRMS errors represent mean values of NRMS errors from all transient time steps for a particular model layer. The following observations can be made from the sensitivity runs:

- Transient model is more sensitive to changes in hydraulic properties than steady-state. Thus, acceptable calibration during steady-state simulation does not guarantee acceptable calibration during transient simulation.
- The model is most sensitive to changes in the hydraulic conductivity and specific storage of Layer 4 (EVA) and Layer 5 (Eastend-Ravenscrag Aquifer). These parameters essentially determine the model's response to any stress.
- The specific storage of Layer 5 (Eastend-Ravenscrag Aquifer) appears to have equal or greater effect on transient calibration than specific storage of the Layer 4 (EVA). At the same time, specific storage of the overlying aquitard (Layers 1 & 2) has no impact on the model, likely due to the low K'_v .
- The model is generally not sensitive to changes in vertical hydraulic conductivity K'_v of Layers 1 and 2 (Drift Aquitard) by a factor of 10, relative to other parameters. However, increasing K'_v by a factor of 100 or more leads to extremely poor steady-state calibration.
- The steady-state model appears to be relatively insensitive to changes in hydraulic conductivity of Layer 3 (Upper Empress). For this reason and to reduce computational time, Layer 3 was combined with Layer 4 during transient sensitivity analysis.

Another important observation from the sensitivity analysis of the transient model is that hydraulic properties of Eastend-Ravenscrag Aquifer appear to have little impact on the transient calibration during the early time of stress but the error increases with time as pumping progresses. This observation can be explained by the fact that during early time of stress, most of the water is extracted from the elastic storage of the EVA. As pumping continues, the increased hydraulic gradient between the EVA and Eastend-Ravenscrag Aquifer generates additional/increasing recharge into the EVA from Eastend-Ravenscrag Aquifer. As a result, model's sensitivity to Eastend-Ravenscrag Aquifer's hydraulic properties increases with time.

The sensitivity analysis has allowed exploration of the range of possible parameter values that may be applied for acceptable calibration within the specified error criteria. Table 11 and Figure 19 document the ranges of hydraulic conductivity and specific storage values that would result in acceptable statistical calibration of this model with NRMS error of $< 10\%$. Based on the better-constrained transient model, the parameters can vary within one order of magnitude or less and still allow for acceptable calibration. The model is entirely insensitive to changes in the specific storage of the Drift Aquitard likely due to its very low hydraulic conductivity.

Table 11: Ranges of Acceptable Parameters Obtained via Sensitivity Analysis

	Drift Aquitard			EVA			Eastend-Ravenscrag Aquifer		
	Steady-state	Transient state		Steady-state	Transient state		Steady-state	Transient state	
	K_v (m/s)	K_v (m/s)	S_s (-)	K_h (m/s)	K_h (m/s)	S_s (-)	K_h (m/s)	K_h (m/s)	S_s (-)
Minimum	1.0×10^{-12}	1.0×10^{-12}	1.0×10^{-12}	3.3×10^{-4}	6.0×10^{-4}	1.0×10^{-6}	5.5×10^{-8}	1.0×10^{-7}	2.8×10^{-5}
Maximum	1.2×10^{-10}	1.8×10^{-11}	1.8×10^{-11}	3.0×10^{-2}	1.5×10^{-3}	2.0×10^{-5}	5.0×10^{-5}	7.5×10^{-7}	4.4×10^{-5}
Calibrated	3.0×10^{-12}	3.0×10^{-12}	3.0×10^{-12}	1.0×10^{-3}	1.0×10^{-3}	1.0×10^{-5}	5.0×10^{-7}	5.0×10^{-7}	4.0×10^{-5}

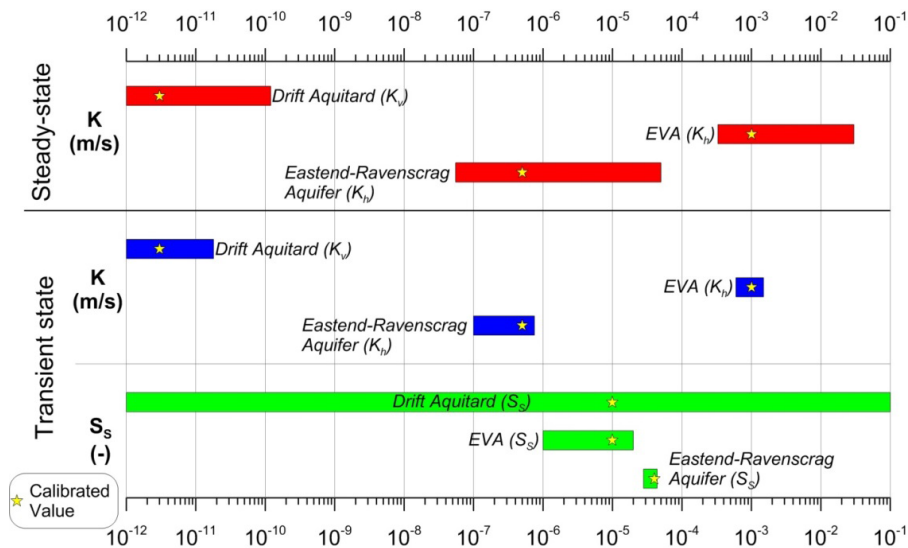


Figure 19: Range of Acceptable Parameter Values Within 10% NRMS Error

4.7 Validation

Uncertainties and assumptions during calibration can lead to non-unique combination of parameters. Consequently, it is possible that calibrated parameters do not adequately describe the aquifer system under a different set of hydrogeologic stresses. Model validation (or verification) is required in order to help establish greater “confidence” in the calibration and overall performance of the model. During validation process, the model is subjected to stresses different from those used for calibration. The aquifer is pumped at different rates, locations, and duration. The results are then compared to the observed data followed by overall assessment of model’s ability to simulate these scenarios.

The groundwater model was able to adequately simulate the recovery after 1994, which points toward adequate validation. This argument is justified because the recovery data from all monitoring wells were intentionally excluded from calibration and thus could not have influenced the parameter estimation process. This is the best evidence for successful calibration of the model. Although some discrepancies between the observed and modelled recovery still exists, this model provides the best recovery prediction when compared to all previous numerical models and is on par with the semi-analytical model by Maathuis and van der Kamp (1998).

Two additional scenarios were examined to validate the model: the 1965-1966 Midale Flowing Shothole and the 1984 Pumping Test. The estimated flow rates and observation data from these events were imported into the existing groundwater model. Boundary conditions and aquifer parameters remained unchanged (i.e. calibrated parameters as per Table 9). Each scenario was modelled separately and results from relevant monitoring locations were compared to the observed response. In general, this model was capable of adequately simulating the drawdown effects of both scenarios and the modelled drawdowns compared reasonably well to the observed drawdowns. The details on the simulation of these scenarios are provided below.

4.7.1 1965-1966 Midale Flowing Shothole

A seismic shothole was drilled on November 20, 1965, at 16-24-04-12W2 (Figure 2) and encountered artesian flow conditions at a depth of 195 ft (Meneley and Whitaker, 1970). Following unsuccessful plugging attempts, it was allowed to flow freely to the surface while taking water level measurements at SRC1U-61 and WSA OUTRAM monitoring wells. The flow was estimated to be between 416 – 1,665 igpm (500 – 2000 USGPM). The shothole was plugged on May 20, 1966, following a total of 182 days of uncontrolled flow. Drawdowns of up to 1 m were measured at SRC1U-61 and WSA OUTRAM monitoring wells followed by slow and incomplete recovery.

This groundwater model was used to simulate the effects of the flowing shothole on monitoring wells SRC1U-61 and WSA OUTRAM (Figure 20) located at respective distances of 15,500 and 25,500 m away from the shothole. It appears that the simulated drawdowns at rate of 500 USGPM (416 igpm) provide very good approximation of the observed drawdowns, particularly at WSA OUTRAM. Rates greater than 416 igpm (500 USGPM) result in overestimated modelled drawdowns. At rate of 832 igpm (1000 USGPM), the modelled drawdowns are over 2 m compared to observed drawdowns of 1 m. Given the uncertainty in the flow rates, it seems reasonable to conclude that in general, this model is capable of adequately simulating the drawdown effects of the flowing shothole at the two monitoring locations.

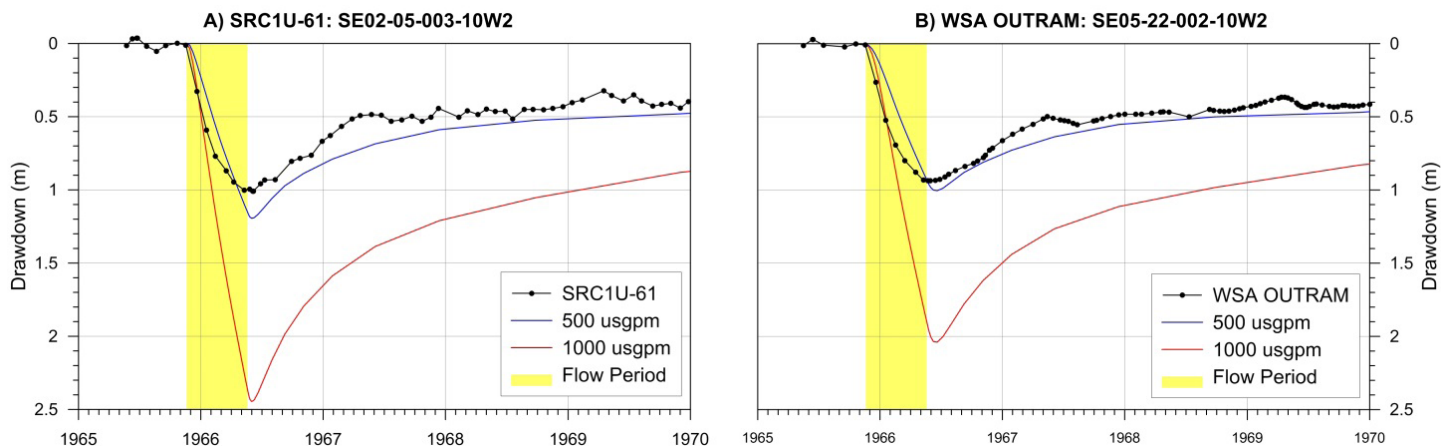


Figure 20: Modelled and Observed Drawdowns at SRC1U-61 and WSA OUTRAM Observation Well in Response to Flowing Shothole at NE16-28-004-12W2

4.7.2 1984 Pumping Test

A long-term pumping test was conducted between September 17 and October 15, 1984, for almost 29 days (28 days and 20 hours). Well PW4UL was pumped at a rate of 6,546 m³/d (1000 igpm) and drawdowns were recorded in 18 monitoring wells (Table 12). Initially, this test was planned for 31 days; however, the pumping stopped early due to a failed transformer during an unexpected snow storm. As a result, there were no measurements taken at the end of pumping period. The last measurements during the pumping test were taken on October 12, 1984. Pumping test data were extrapolated until October 15, 1984 using figures from van der Kamp (1985) and analytical solutions. Recovery measurements were collected until August 2, 1985.

The model grid was refined around the pumping well to reflect the distances between pumping and monitoring wells and the model was then run to simulate the effects of this pumping test. The comparison of observed and simulated drawdowns at selected wells is shown on figures in Appendix D and the differences between maximum drawdowns are summarized in Table 12 and Figure 21. The majority of residuals are less than 1 m, with exception of wells M10U-82 and M19U-84. Overall, the model appears to be capable of simulating the effects of this pumping test.

The differences between modelled and observed drawdowns in some wells can be attributed to variations in the transmissivity within the EVA. Pumping well PW4UL was screened across the entire aquifer while monitoring wells can target individual sand intervals within aquifer. For example, monitoring well M09L-82 is screened in the lower sand of EVA and M10U-82 is screened in the upper sand of EVA. While both wells are located at similar distance away from the pumping well, the M10U-82 well has greater drawdown than M09L-82. Another example is the greater drawdown in well M13UL-84 than in well M12UL-84 (both wells completed in the upper and lower sands of EVA), despite the fact that well M13UL-84 is located further away from pumping well than well M12UL-84.

Table 12: List of Monitoring Wells and Drawdowns During 1984 Pumping Test

Well ID	Distance from Pumping Well (m)	Max Drawdown (m)		Residual (m)
		Observed*	Model	
PW4UL**	0	44.0	-	
M15IT-84	30	0	-	
M14IT-84	30	0.4	-	
M12UL-84	30.5	8.8	9.4	-0.6
M13UL-84	98.8	9.4	8.7	0.7
M09L-82	323	7.6	7.8	-0.2
M10U-82	323	9.2	7.8	1.4
M17U-84	1,510	7.3	6.5	0.8
M16R-84	2,200	0	-	-
M19UL-84	3,500	7.6	6.3	1.3
SRC1U-61	5,375	0	-	-
M11L-84	5,250	4.6	4.4	0.2
M06L-82	7,300	4.2	3.5	0.7
M04U-82	8,651	0.4	1.0	-0.6
TW1L-65	8,625	0.4	1.0	-0.6
M20U-84	11,700	3.8	3.5	0.3
M18UL-84	13,000	2.4	2.8	-0.4
M07U-82	22,000	0	-	
GSC3AL-60	22,000	0	-	

*Extrapolated using analytical solutions and figures from van der Kamp (1985).

**This well was originally named PW2UL and renamed to PW4UL in 1988.

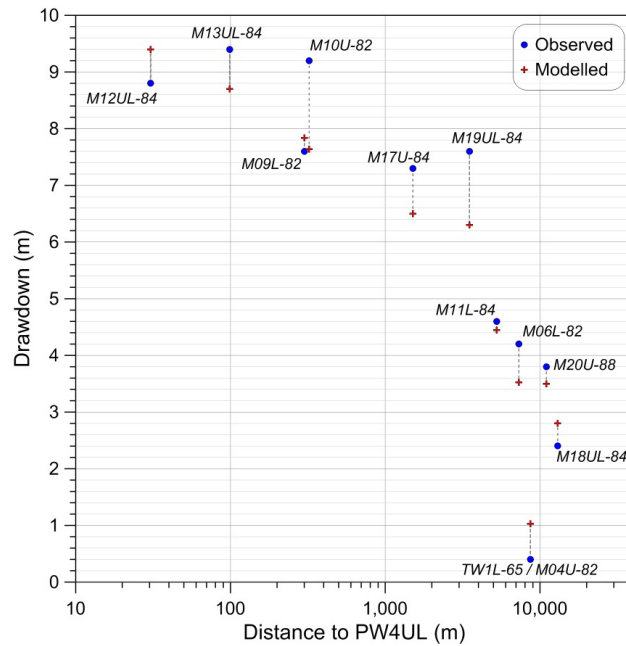


Figure 21: Distance-Drawdown Plot of the Observed and Modelled Maximum Drawdowns During the 1984 Pumping Test of PW4UL-84

4.8 Implications on Conceptual Model

Van der Kamp et. al. (1986) used water level measurements from the Weyburn Channel to estimate the bulk vertical hydraulic conductivity (K'_v) of thick tills. Their work has demonstrated that K'_v of thick tills in the Weyburn area is likely within a range of $10^{-10} - 10^{-9}$ m/s. All historical models used vertical hydraulic conductivity ranging between $2.7 \times 10^{-10} - 5.7 \times 10^{-9}$ m/s (Table 1). The present model has suggested that the bulk vertical hydraulic conductivity of the overlying till may be 3×10^{-12} m/s or lower. This is at least two orders of magnitude lower than previously considered values for this area but within the ranges presented by Freeze and Cherry (1979) and Domenico and Schwartz (1990). Such low K'_v of till would imply that little to no vertical recharge is actually reaching the EVA. Based on this study, it appears that the aquifer is recharged mostly laterally from the Eastend-Ravenscrag Aquifer. Transient sensitivity analysis (Appendix C) indirectly shows that there is long-term interaction between the EVA and the bedrock. The discharge area of the EVA is unknown.

While sensitivity analysis presents compelling qualitative evidence for adequate calibration, it does not account for the possibility of existence of a completely different conceptual model. Given the anomalously low value of K'_v obtained from calibration, it became necessary to consider the possibility of alternative conceptual model. Based on our judgement, this alternative scenario could definitively test whether the obtained parameters are unique. In this scenario, the K'_v of till was increased to $10^{-10} - 10^{-9}$ m/s which is within the historical range of values. This constraint is critical since the goal of this scenario is to test whether a successful and meaningful calibration can be obtained using these historical parameters. In order to compensate for the increased recharge through till, the lateral hydraulic conductivity of Layer 5 (Eastend-Ravenscrag Aquifer) was reduced to 10^{-12} m/s. Hydraulic conductivity of Layer 5 could gradually be increased/adjusted if found necessary. Hydraulic properties of the EVA and boundary conditions were not changed. This simplified conceptual model implies that EVA is encased in aquitards laterally and below with most of the recharge controlled by hydraulic conductivity of overlying till and boundary conditions within the EVA.

Steady-state and transient simulations were calibrated resulting in a K'_v value of 5×10^{-10} m/s of the Drift Aquitard. The modelled steady-state hydraulic heads were matching reasonably well to the distribution of observed pre-pumping hydraulic heads. The steady-state NRMS error was calculated to be 5% and the average transient NRMS error was calculated to be 6.2%, both of which are considered acceptable.

The resulting hydrographs of WSA ESTEVAN and WSA OUTRAM are shown on (Figure 22). The alternative model approximates the general trend reasonably well during 1988 – 1992 period, when the pumping rates were increasing and water levels decreasing. The pumping rates were reduced between 1992 – 1994 and the model predicted increase in water levels (mild recovery). However, the observed water levels showed no recovery and remained relatively constant during the last two years of production, even with the reduced pumping rates. Lastly, the model of the alternative scenario predicted nearly complete recovery approximately 2 – 3 years after cessation of pumping. This was not the case since the recovery still continues today, 22 years since the pumping stopped.

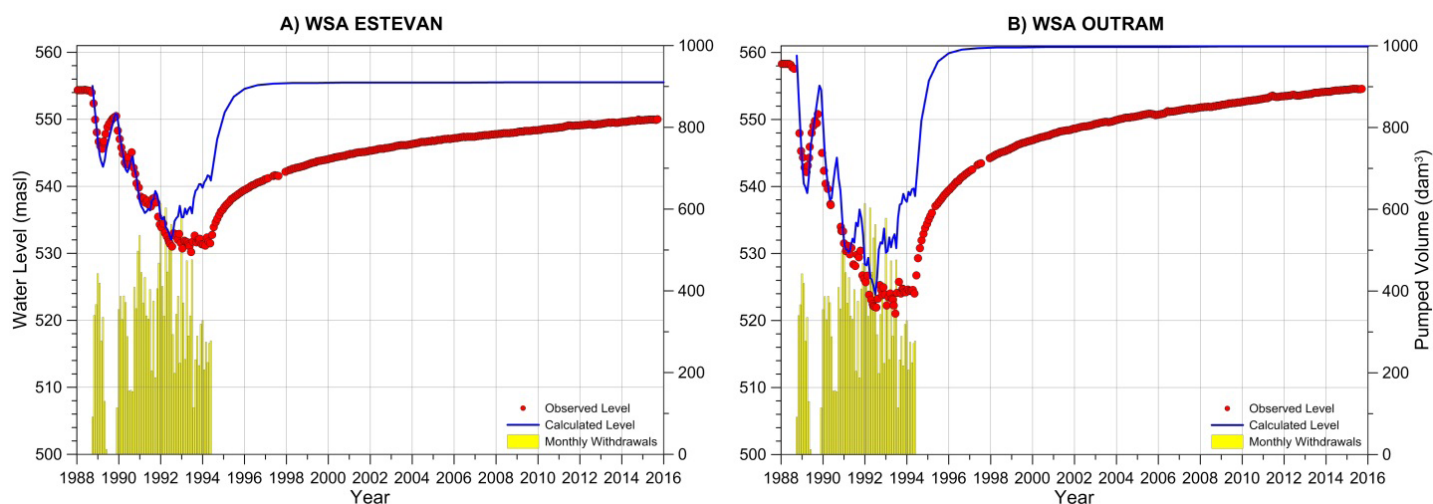


Figure 22: Simulated Response of Monitoring Wells due to Alternative Transient Scenario

Neither boundary conditions nor other aquifer parameters in the alternative scenario could be varied within reasonable range to obtain a better transient match. Increasing hydraulic conductivity of Layer 5 (Eastend-Ravenscrag Aquifer) to a more reasonable value while maintaining high aquitard K'_v of $10^{-10} - 10^{-9}$ m/s would only result in greater recharge and even faster recovery. Thus, the results of the simulation of the alternative scenario demonstrate that K'_v of $10^{-10} - 10^{-9}$ m/s did not result in adequate calibration to the pumping water levels, particularly at a later pumping time. K'_v of till must be further reduced to 3×10^{-12} m/s while increasing hydraulic conductivity of bedrock in order to provide some recharge into the EVA.

Conceptually, the extremely low hydraulic conductivity of the till implies that the EVA is a relatively isolated aquifer recharging mostly through the Eastend-Ravenscrag Aquifer. EVA acts as a high-conductivity conduit for the water from bedrock as described by Meneley (1983). This also implies that the drawdowns are unlikely to impact surface water.

4.9 Predictive Simulations and Aquifer Yield

The sustainable yield of an aquifer is the amount of water that can be withdrawn from an aquifer without producing undesirable results (Maathuis and van der Kamp, 1998). This implies that the recharge, discharge and the net change in storage must reach new and acceptable equilibrium in steady-state scenario. From a practical perspective, the main criterion for steady-state sustainable yield in the EVA is such that the water levels remain above the top of the aquifer. Using this definition, Maathuis and van der Kamp (1998) estimated that sustainable yield of EVA is between 2,400 – 2,800 dam³/year assuming drawdown of 45 m around the well field. At these rates, they estimated that steady-state drawdown at R3UL (Yellowstone Channel at the international border) and R6UL (eastern part of the Estevan Valley) will be in the order of 25 – 33 and 22 – 28 m, respectively.

The main objective of the present model is to gain ability to simulate various pumping scenarios and their effect on water levels, including steady-state situation (if such is ever achieved). In order to address this goal, the model was run in transient state for 1, 5, 10, and 20 years in order to determine optimal withdrawal while maintaining water levels above the top of the aquifer. The last simulation was performed in steady-state in order to establish the sustainable yield of the EVA.

The following assumptions were made herein in order to simulate pumping scenarios:

- All scenarios considered a similar well configuration consisting of four pumping wells that were used by SaskPower during 1988 – 1994 withdrawals.
- The available head for all four wells was assumed to be 55 m (Table 13). This is the value of available head in well PW4UL-88 which is the lowest and limiting value for the entire well field.
- Upper Empress and EVA (Layers 3 and 4) form a single aquifer. Consequently, aquifer top is the top of Layer 3.
- Each well was pumped at equal pumping rates. Actual pumping rates will depend on well efficiency and capacity of each well. The ultimate goal of presented simulations is to estimate the total withdrawal rate from the system (i.e. sum of all four wells) while ensuring that drawdowns do not exceed the available head of 55 m.

Table 13: Available Drawdown in the Production Wells

Well	Surface Elevation (masl)	Static Water Level (masl)	Aquifer Top (masl)	Available Drawdown (m)
PW1U-88	569.32	557.24	494.19	63.05
PW2U-88	572.68	557.13	477.58	79.55
PW3UL-88	566.00	556.10	498.03	58.07
PW4UL-88	563.44	556.39	501.56	54.83

The model was run iteratively by varying pumping rates for each time scenario until the drawdown around pumping wells was approximately 55 m (Table 14). The greatest drawdowns are expected once the system reaches steady-state (Figure 23). Using the calibrated parameters from Table 9, steady-state simulations have estimated the sustainable aquifer yield to be 1,800 dam³/year. However, this value does not account for variations in the aquifer properties. For this reason, the model was run multiple times while varying the parameters within the maximum and minimum ranges as outlined by the sensitivity analysis (Table 11). Only one parameter was varied at a time while the rest were kept at their calibrated values. This resulted in sustainable yields ranging from 1,200 to 2,100 dam³/year. This suggests that the EVA can be pumped indefinitely at a rate within the 1,200 – 2,100 dam³/year range. However, caution should be exercised when using the steady-state sustainable yields due to the dependency of the steady-state model on uncertain boundary conditions.

The sustainable yield predictions of the steady state model are lower than earlier predictions of 2,400 – 2,800 dam³/year by Maathuis and van der Kamp (1998). However, the transient scenarios show that the aquifer can be pumped at much greater rates for shorter periods of time (Table 14). For example, the EVA could be pumped at rates of 6,200 dam³/year for up to five (5) years. This scenario has more practical value and suggests that SaskPower's average withdrawal rate of 4,143 dam³/year during 5.15 years of pumping was below the sustainable yield for that period of time. However, the transient model also suggests that pumping at this rate for longer than 12.6 years would not be sustainable and the water levels would have dropped below aquifer's top at the production site (Figure 24).

It should be noted that the transient scenarios also show that the aquifer can be pumped at rate as high as 10,800 dam³ for up to one (1) year. However, pumping at such high rates may produce higher than expected drawdowns in the pumping wells due to well losses. Withdrawal rates should be reduced if the aquifer is to be pumped for longer periods. Cumulatively, more water can be withdrawn if the aquifer is pumped at lower pumping rates but for longer periods. In general, transient drawdowns at the monitoring wells increase with longer pumping time.

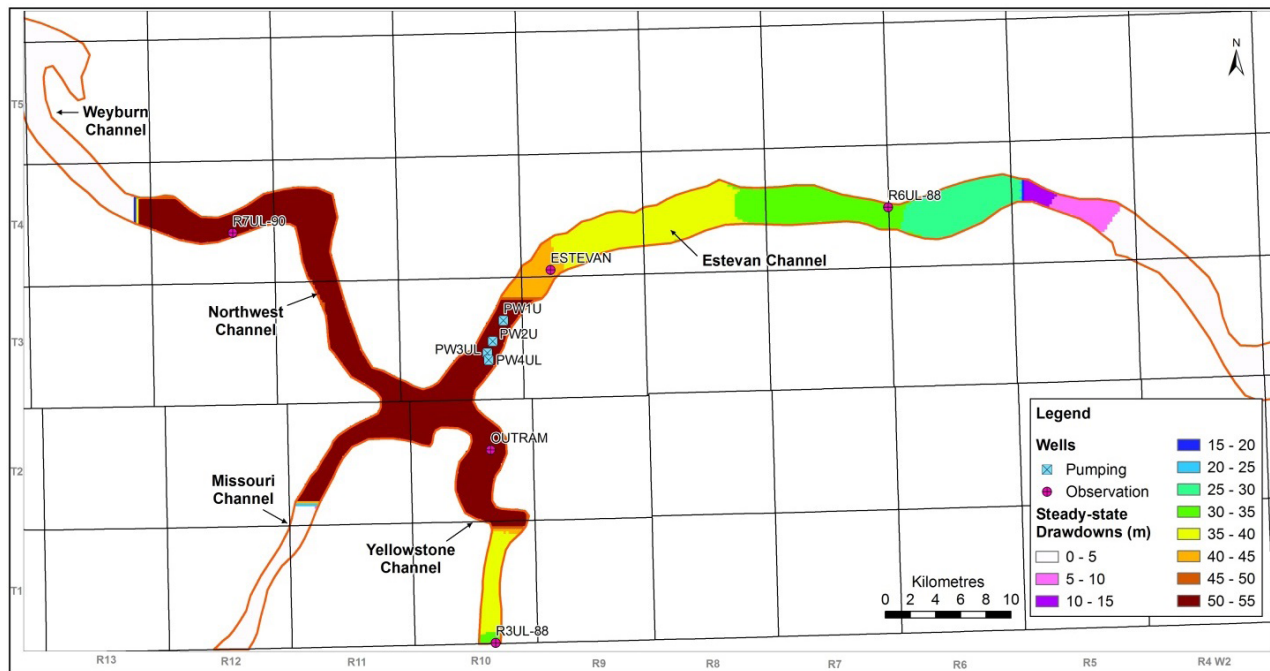
Table 14: Pumping Scenarios Using Four Existing Production Wells

Time	Total Pumping Rate (dam ³ /year)	Cumulative Volume (dam ³)	Drawdowns**					
			Pumping Wells* (m)	WSA Estevan (m)	WSA Outram (m)	R3UL (m)	R7UL (m)	R6UL (m)
1 year	10,800	10,800	55	23.0	41.1	21.2	17.1	8.0
5 years	6,200	31,000	55	30.4	45.5	25.2	31.5	16.5
10 years	4,800	48,000	55	32.5	46.7	27.1	36.8	19.5
20 years	3,800	76,000	55	35.6	49.3	29.8	42.7	23.4
Steady-State	1,800	∞	55	40.5	52.7	34.8	52.1	30.5

*Lowest available drawdown (distance between static water level and aquifer top at well PW4UL-88)

**See Figures E.1-E.5 for detailed drawdown distribution for each scenario

Figure 23: Distribution of Steady-State Drawdowns While Pumping at Rate of 1,800 dam³/year



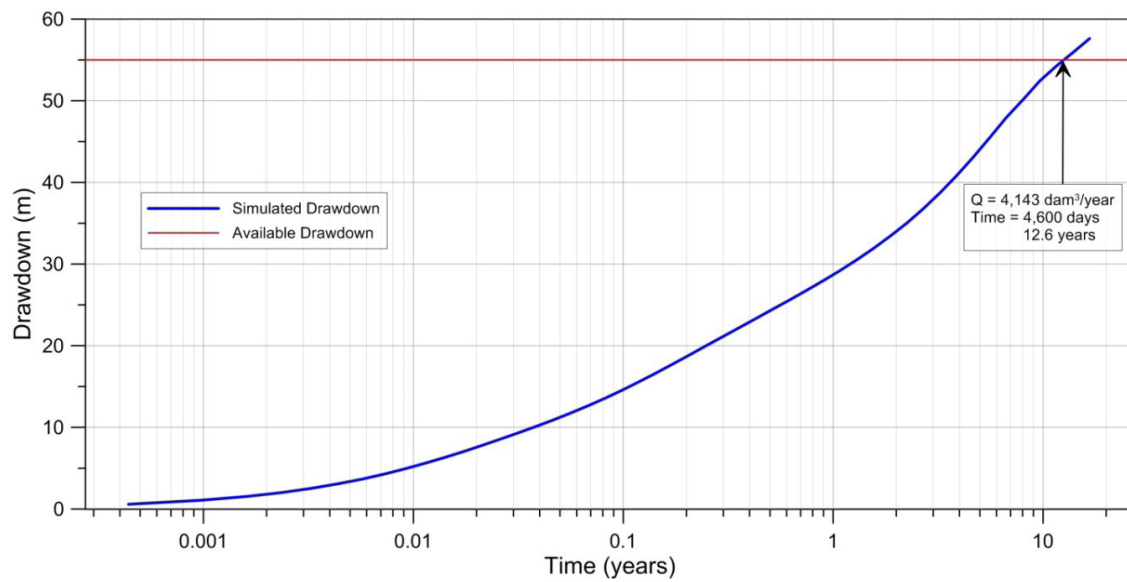


Figure 24: Simulated Drawdowns at the Centre of SaskPower's Wells Field Using Average Rate of 4,143 dam^3/year .

5.0 Summary

The Estevan Valley Aquifer (EVA) is located north-west of Estevan, sits in a deep (50 – 150 m), relatively narrow, and long (> 100 km) paleo-valley and consists of interbedded sand, gravel, silt, and clay. Although it has been mapped and explored since the late 1950's, its long-term yield remains unclear. SaskPower pumped this aquifer between 1988 – 1994 at average rate of 4,143 dam³/year and produced extensive drawdowns throughout most of the aquifer and across the international border within the Yellowstone Channel. More importantly, the response of the water levels in the aquifer showed that previous research and models have overestimated the sustainable yield and pumping at this rate is not sustainable in the long-term.

A finite-difference groundwater model was developed herein to assist WSA staff in assessing the availability of groundwater resources in the EVA and predicting aquifer response from various pumping scenarios. The groundwater model was refined by incorporating geological and hydrogeological information up to 2016. Geological and hydrogeological information included compilation of available testholes, piezometers, production wells, withdrawal data, and water level measurements that have become available since the 1960's and the geologic surface has been refined with the updated information.

The groundwater model redefined our understanding of the EVA hydraulics. Calibrated values of the bulk vertical hydraulic conductivity (K'_v) of the overlying tills range between 10^{-11} – 10^{-12} m/s, which is at least two orders of magnitude lower than previously considered for this area. Such low K'_v of till would imply that direct contribution of recharge into the EVA across the overlying drift aquitard is relatively small. The aquifer is; therefore, recharged mostly laterally from the adjacent Eastend-Ravenscrag aquifer. The discharge area of the EVA remains unknown.

The groundwater model was calibrated to the observed drawdowns during the 1988 – 1994 pumping period. Transient calibration has shown that model is capable of adequately simulating stresses through most of the EVA, except at the international border in the Yellowstone Channel. The poor calibration result at the international border is likely due to uncertainties in geology and the associated boundary conditions. The simulated recovery is overestimated during early time and underestimated at late time. In general, the model agrees with the observations of long and slow recovery as indicated at wells WSA ESTEVAN and WSA OUTRAM.

Sensitivity analysis was completed by varying aquifer and aquitard parameters within reasonable ranges to ensure that the combination of calibrated parameters is unique. Model's performance was validated using different set of stresses. Simulated response to Midale flowing shothole and the 1984 pumping test showed that the model is capable of predicting drawdowns from stresses at varying rates, locations, and duration. Simulation of the 1984 pumping showed the presence and emphasized the effects of heterogeneities within the EVA at local and regional scales.

The model was tested using short- and long-term pumping scenarios using SaskPower's four wells. The aquifer was stressed such that water levels remained above the top of the aquifer with an available drawdown of 55 m in proximity of the pumping wells. Using the steady-state simulation, the long-term sustainable yield was estimated to be 1,800 dam³/year and a possible range of 1,200 – 2,100 dam³/year based on sensitivity analysis. The model was then run in transient state for 1, 5, 10, and 20 years in order to determine optimal withdrawal rates. The determined combined pumping rates were 10,800 dam³/year, 6,200 dam³/year, 4,800 dam³/year, and 3,800 dam³/year, respectively. This approach can be used in the future to estimate pumping rates from withdrawal wells

located elsewhere along the aquifer. The greatest value of this work lies in the ability of the model to simulate transient changes. Transient model can provide initial estimate of the expected drawdowns for any requested allocation assuming that duration of withdrawal is known. In applicable terms, this means that any future allocations should consider the life span of a particular project and its long-term impacts.

5.1.1 Recommendations

Despite the abundance of data relative to other aquifers in Saskatchewan, uncertainties remain in the geology of the EVA leading to simplified aquifer representation at the boundary conditions and throughout the aquifer. While field investigations could improve our understanding of EVA, any new test drilling would have to be carefully considered and likely be based on the results of preceding geophysical investigations. Pumping tests of the EVA elsewhere along the channel could also provide additional insight into the effects of hydraulic discontinuities and hydraulics of the aquifer, particularly in the Yellowstone Channel.

Other recommendations from this work include:

- Examine and compare groundwater quality from the EVA and adjacent aquifers in order to assess the recharge contribution from various aquifers/aquitards to the EVA. This may include detailed desktop review of existing water quality as well as additional groundwater sampling for major ions and environmental isotopes (Lo and Melnik, 2017).
- Incorporation of additional data from North Dakota will allow to effectively extend the model south moving the boundary condition further away from international border.
- Improve model's calibration at the international border and gain greater confidence in the estimate of the sustainable yield of the aquifer.

6.0 References

- Beckie, V.C., and Pasloske, G.R. 1985. Estevan Valley aquifer system. Exploration and pump test program Souris River site – 1984. Beckie Hydrogeologists Ltd., Regina, 38 p.
- Beekly, A.L. 1912. The Culbertson lignite field, Valley County, Montana: United States Geological Survey, Bulletin 471, pp 319-358.
- Christiansen, E.A., 1968, Pleistocene stratigraphy of the Saskatoon area, Saskatchewan, Canada, Canadian Journal of Earth Sciences, 5: 1116-1173
- Christiansen, E.A., 1983, Geology of the Eastend to Ravenscrag formations, Saskatchewan. In Meneley, 1983. Hydrogeology of the Eastend to Ravenscrag formations in southern Saskatchewan. Report #0088-001.
- Domenico, P.A. and Schwartz, F.W., 1990. Physical and Chemical Hydrogeology. John Wiley & Sons, New York, 824 p.
- Freeze, R.A., and Cherry, J.A., 1979. Groundwater. Englewood Cliffs, Prentice-Hall, New Jersey, 604 p.
- Keller, C.K., van der Kamp, G., and Cherry, J.A., 1989. A multiscale study of the permeability of a thick clayey till. Water Resources Research, Vol. 25, No. 11, pages 2299-2317, November 1989.
- Komex, 2003. Geophysical surveys, Weyburn, Saskatchewan, buried preglacial Weyburn valley. Komex International Ltd., prepared for Saskatchewan Research Council, report # C57350000, 23p.
- Lo, K., and Melnik, A., 2017, Water chemistry and natural tracer analysis, (Regina area aquifers), Water Security Agency, Internal investigation, 28 p.
- Lu, F. and Jin, Y.C. 2002. Groundwater Modeling for the Estevan Valley Aquifer – A case Study. In 55th Canadian Geotechnical and 3rd joint IAH-CNC and CGS Groundwater Speciality Conference, Niagara Falls, October 2002.
- Maathuis, H., and Simpson., M.A., 2003a. Delineation of the Weyburn Valley aquifer in the “Local” IEA Weyburn CO2 Monitoring Area, Saskatchewan. IEA Weyburn CO2 Monitoring Project Task 2.2.5. Saskatchewan Research Council, Publication No. 11634-1E03. 17 p.
- Maathuis, H., and Simpson., M.A., 2003b. Regional Hydrogeology of the Weyburn CO2 monitoring project area IEA Weyburn CO2 Storage and Monitoring Project: Task 2.2.3 - Regional “Shallow” Hydrogeology. Saskatchewan Research Council, Volume I: Text. Publication No. 11510-1E03, 45 p.

Maathuis, H., and van der Kamp, G. 1989. Preliminary evaluation of the Estevan Valley and Tableland aquifer (Draft). Saskatchewan research council, Publication R-1220-2-R-89, 64 p.

Maathuis, H., and van der Kamp, G., 1998. Evaluation of pumping and recovery data for the Estevan Valley and Tableland aquifers. Saskatchewan Research Council, publication no. 10421-1C98.

Meneley, W.A., Christiansen, E.A., and Kupsch, W.D., 1957. Pre-glacial Missouri River in Saskatchewan. *Journal of Geology*, Vol. 65 pp 441-447.

Meneley, W.A., and Whitaker, S.H., 1970. Geohydrology of the Moose Mountain upland in southeastern Saskatchewan. Saskatchewan Research Council, publication G-70-1, 52 p.

Meneley, W.A. 1972. Groundwater – Saskatchewan. *In* Water supply for the Saskatchewan Nelson Basin, Saskatchewan – Nelson Basin report, Ottawa, Appendix 7, Section F, 673-723 pp.

Meneley, W.A., 1983. Hydrogeology of the Eastend to Ravenscrag formations in southern Saskatchewan. W.A. Meneley Consultants Ltd., Report 0089-001, 21 p.

Neville, C.J., and van der Kamp, G. 2012. Using recovery data to extend the effective duration of pumping tests. *Groundwater*. 50:804-807.

Puodziunas, P.P. 1977. Souris River basin groundwater study – Saskatchewan. Saskatchewan Research council, Geology Division, report G-77-3, 63 p.

Schreiner, B.T., 2010. Geology and groundwater of southern Saskatchewan, Hydrogeologic mapping protocol. Saskatchewan Research Council, publication no. 12831-1E10.

Simpson, M.A., 1993. Geology and groundwater resources of the Weyburn/Virden area (62E/F), Saskatchewan. Saskatchewan Research Council, publication no. R-1210-3-E-93.

Simpson, M.A., 1996. Aquifer mapping in southeast Saskatchewan using transient electromagnetic soundings. Saskatchewan Research Council, Publication G-744-2-C-83, 49 p.

van der Kamp, G. and Schneider, A., 1983. Computer model for a buried-valley aquifer near Estevan, Saskatchewan. Saskatchewan Research Council, Publication G-744-2-C-83, 49 p.

van der Kamp, G. 1985. Yield estimates for the Estevan Valley aquifer system using a finite-element model. Saskatchewan Research Council, Publication R-844-4-C-85, 49 p.

van der Kamp, G., 1989. Calculation of constant-rate drawdown from stepped-rate pumping tests. *Ground Water* Volume 27, pp. 175-183.

van der Kamp, G., Maathuis, H., and Meneley, W.A. 1986. Bulk hydraulic conductivity of a thick till overlying a buried-valley aquifer near Weyburn, Saskatchewan. *Proceedings of Third Canadian Hydrogeological Conference, IAHC-CNC, Saskatoon, April 20-23, 1986*, pp. 94-99. Van Stempvoort, D.R. and Simpson, M., 1994. *Hydrogeology of the southeast aquifer management plan area. Volume 1: text (revised in January 1995). Volume 2: maps, cross-sections and diskettes.* Saskatchewan Research Council, Publication R-12202-9-E-94, 223 p.

van der Kamp, G., and Maathuis, H. 2012. The unusual and large drawdown response of buried-valley aquifers to pumping. *Groundwater*. 50:207-215.

Walton, W.C. 1965. Potential yield of a sand and gravel aquifer in a buried valley near Estevan, Saskatchewan. Results of aquifer and well production tests and evaluation of aquifer potential. W.C. Walton, consulting groundwater-water hydrologist, Urbana, Illinois. Report prepared for the Saskatchewan Research Council, 45 p.

Whitaker, S.H., and Christiansen, E.A., 1972. The Empress Group in southern Saskatchewan. *Canadian Journal of Earth Sciences*, Vol. 9, pp 353-360.

Appendix A: Geologic Maps and Cross-Sections

Appendix B: Hydrographs of Calibrated Model

Appendix C: Sensitivity Analysis

Appendix D: Hydrographs of 1984 Pumping Test

Appendix E: Simulated Drawdown for Various Transient Scenarios